UNIVERSIDADE DE LISBOA
Faculdade de Ciências
Departamento de Química e Bioquímica

INVESTIGATING DEPENDENCIES OF RAS MUTANT LUNG CANCER CELLS

Nádia Sofia de Carvalho Lima

Dissertação orientada por Prof. Doutor Julian Downward
e Prof. Doutor Carlos Farinha

MESTRADO EM BIOQUÍMICA
Bioquímica Médica
Dissertação
2015

Acknowledgements

First, above all and everyone I am grateful to Prof. Doctor Julian Downward. For the incomparable and unique opportunity he gave me when I joined his Lab. I was blessed to get to grow at many levels in such environment, full of great and intense debates with the most intelligent and admirable scientists, promptly helpful people with infinite good characters. I will always and ever feel flattered to deserve your confidence since the first minute. My life would not have the same value without this experience.

To Alice Zhou, my closer supervisor. She shared with me all her knowledge, helped me since the first moment and made me always believe that sometimes what seems to be impossible can be turned into something real. We were truly a team! Her friendship and care about me were beyond my expectations. Thank you Alice for being part of my life this year.

To all my lab colleagues, a special acknowledgement to Miriam, the "brain and expertise" of the lab. With her wide knowledge, in a blink of an eye, she always knows how to carry on in science, I truly respect you. To Clare, the most funny and wise lady in the entire world, a friend that never let me down and always carried me. We shared great moments! To Davide, the listener and the most working-hard scientist with the best taste in music. And to all the others a big thank you for sharing 9 months of your life with me. For all those Fridays I was dragged from the lab to share "happy pints" as the British style while having interesting conversations...

To my friends in London, Julie and Juliana. We shared not only a house but a life. For all those nights I arrived home completely brainless and you still managed to put a smile on my face... Thanks for listening to my stories about spheres, tumors and stubborn western blots very patiently and for making me believe in myself. Also, a special thank you to my dear friends in Portugal, Maguiezita, Catarinazinha, Marlene and Cris.

Finally, to my mother, the one who was always there, unconditionally every minute of my life. To my father who never says a word but I know that he is deeply proud of me! And to my brother that always find a way of explaining my scientific achievements with an artistic touch.

Because of all the questions I still want to explain and because "if you can't explain it simply, you don't understand it well enough" (Albert Einstein), I will always be an excited and ambitious scientist.

To myself and to my mother...

Abstract

Lung cancer is a leading cause of death worldwide. Genetic features like *KRAS* mutations are known to be a risk factor. The GTPase switcher RAS takes part on many aspects of the cell pathway and signal transduction. Example of that is its recognized involvement in cell survival, proliferation, metabolism, motility, immune response and many others. RAS constitutive activation driven by the common G12D *KRAS* mutation is responsible for numerous cancer hallmarks.

To date, direct target of the mutant KRAS is still poorly efficient. Despite all the efforts and continuous advances in targeting either upstream and downstream KRAS effectors, there is still a long path to be taken with dubious questions to be answered. Several inhibitors are already in clinic, however the ability of RAS to compensate targeted pathways, and activate other effector kinases reduces their efficiency in the clinical setting. Other difficulty in the drug development field is to extrapolate the *in vitro* results to *in vivo* predictions. In this regard, 3D cultures are known to better model the *in vivo* situation than the frequently used 2D cultures. *In vivo* morphologic, physiologic, pathologic and functional environmental features of the tumor biology are aspects that can be simulated by 3D models, better predicting and evaluating therapeutic outcomes.

In this work, 3D culture models of NSCLC (non-small cell lung cancer) cell lines have been developed along with an appropriate method to monitor cell viability in spheroids. The presence of an artificial extracellular matrix is shown to support proliferation and survival of NSCLC, promoting a non-anchorage independent multicellular growth. 3D models are also shown here to encourage cell structural organization and differentiation. Besides, the activity of p-ERK is especially elevated in these systems. A metabolic ATP-based viability test integrated with an efficient cell lysis is described as being an efficient, sensitive and accurate tool to evaluate the viability of spheroids. It is also shown that 2D and 3D culture cells have different sensitivities to drug treatments. Whereas 3D cultures are mostly vulnerable to structural stability disruption and PKC inhibition, 2D cultures show increased sensitivity upon MEK inhibition.

Nevertheless, vulnerabilities and KRAS dependency is cell line dependent and variability can be found between 2D and 3D models. However, results do not diminish the importance of using 3D cultures as valuable platforms to get better *in vivo* therapeutic predictions. It can eventually be the tool we are lacking to find new target therapies. It is therefore still a work in progress awaiting for a large-scale drug screen in order to highlight potential 3D exclusive drug candidates.

Keywords: 3D cell culture; spheroid viability assay; lung cancer; NSCLC; KRAS pathway inhibition; drug screening.

Resumo

O cancro do pulmão é uma das principais causas de morte no mundo. Só em 2012 na Europa cerca de 388.000 mortes foram registadas. Apesar da existência de algumas drogas eficazes para o tratamento do cancro do pulmão, o reaparecimento da doença é frequente após o tratamento. A aquisição de mutações pontuais que causam resistência e aparecimento de vias de sinalização alternativas e compensatórias é a principal causa.

Apesar da conhecida associação do cancro do pulmão com o tabagismo, outros fatores de risco são conhecidos. Entre os principais, conta-se a história familiar. Alterações genéticas incluem na maioria dos casos mutações nos genes *p53*, *Bcl2*, *Rb, FHIT* e $p16^{INK}$. Perda de heterozigotia, mudanças em telomerases e a ativação constitutiva do oncogene *KRAS* são também evidentes fatores de risco.

Dentro do vasto painel de mutações para *KRAS*, pode contar-se como mais comum a G12D, responsável pelo desenvolvimento do subtipo cancro do pulmão de células não-pequenas (NSCLC), um dos mais agressivos.

A proteína RAS é codificada pelo gene *KRAS*. Pertence à família das GTPases e tem como função molecular a ativação e desativação por fosforilação de GDP a GTP e vice-versa. Está envolvida numa longa cascata de transdução do sinal responsável pela proliferação e sobrevivência celular. As mutações em KRAS têm portanto um papel fundamental no aparecimento e desenvolvimento do cancro. A sua ativação constitutiva leva à continua estimulação das vias de sinalização a jusante promovendo a constante proliferação e sobrevivência, reprogramação metabólica, reorganização do citoesqueleto, inflamação e remodelação do microambiente para adaptação tumoral.

Até à data, a direta inibição do mutante $KRAS^{G12D}$ tem-se revelado impossível. Contudo, a proteína RAS encontra-se no topo de uma bifurcação de sinalização, tendo como principais alvos cinases como RAF, MEK, AKT e PI3K. Deste modo, alguns inibidores têm sido desenvolvidos nos últimos anos com o objetivo de bloquear alguns destes efetores tanto a montante como a jusante das vias de sinalização RAS. Inibidores das proteínas MEK e PI3K são dois casos já

clinicamente aprovados. Contudo, os progressos têm sido frequentemente atenuados devido à enorme capacidade da proteína RAS em alcançar inúmeras vias de sinalização alternativas e compensatórias, apontando para a necessidade do uso de terapias combinadas.

O laboratório de Julian Downward, tem reunido esforços valiosos para a identificação de dependências exclusivas do mutante KRAS. A título de exemplo foi demonstrado que os inibidores MEK são seletivamente tóxicos para o mutante KRAS, enquanto o mesmo já não acontece para os inibidores de PI3K. Complementarmente, foram identificadas algumas dependências seletivas do mutante KRAS para atividades que não são diretamente reguladas pelo oncogene RAS. O mutante KRAS é por exemplo dependente da cinase de ligação 1 (TBK1), da cinase-1 ativada pelo fator de crescimento transformador β (TAK1), do fator de transcrição GATA2, da ciclina dependente de cinases CDK4, de alguns reguladores mitoticos, componentes do proteassoma entre outros.

A grande maioria do conhecimento científico adquirido nesta área foi desenvolvido em culturas celulares em mono-camada com linhas celulares originárias de tumores de pacientes. Contudo, a sua manutenção prolongada em cultura conduz a um inevitável estado de adaptação e dependência gerados pela adição continua de suplementos ao meio de cultura. Este ambiente artificial leva à acumulação de mutações, e quando comparadas com células *in situ*, diferenças a nível molecular como diferentes expressões de marcadores de diferenciação, adesão e recetores de fatores de crescimento, podem ser encontradas. A credibilidade destes métodos em representar o tumor original e a confiança com que podem fornecer informações acerca de previsões clinicas começa então a ser posta em causa.

O desenvolvimento de novos fármacos requer modelos que possam simular exatamente as condições *in vivo* e que possam ter relevância clínica. Desta forma, os modelos de cultura tridimensionais (3D) têm ganhado ênfase dentro da comunidade científica devido à sua capacidade em reproduzir a situação *in vivo*. Estas são conhecidas por manter o fenótipo de células tumorais funcional e copiar características morfológicas, fisiológicas, patológicas e ambientais do tumor. A organização de uma estrutura multicelular e o microambiente envolventes têm um impacto notório na sobrevivência e progressão tumoral. Estes têm também um papel fundamental na expressão genética, fenótipo e resposta/sensibilidade a diferentes inibidores terapêuticos. As culturas 3D são capazes de abranger todas estas características, eliminando

algumas das desvantagens presentes nas culturas bidimensionais (2D). São portanto uma ferramenta bastante promissora no que diz respeito ao desenvolvimento rápido de novas terapias, diminuindo custos de estudos preliminares e indo de encontro ao progresso farmacêutico e clínico.

Neste projeto, dado as descritas vantagens dos modelos 3D, foi desenvolvido um método 3D que permita o crescimento e sobrevivência celular de NSCLC conjuntamente com um método que permita a monitorização da viabilidade celular em esferoides. Seguidamente, tendo em conta as vulnerabilidades da mutação KRAS e as suas dependências já mencionadas anteriormente, foram realizados testes de comparação 2D e 3D com o intuito de averiguar quão dependente a via de sinalização RAS é do método de cultura implementado. Pretendeu-se estudar que tipo de diferenças morfológicas, de sinalização e sensibilidade a inibidores existiam que pudessem conferir maior sensibilidade a culturas 2D ou 3D.

Vários métodos de cultura celular 3D já são conhecidos. Suspensões celulares podem ser usadas principalmente para formar simples aglomerados celulares. Superfícies antiaderentes são uma opção, assim como a técnica da *hanging-drop*, onde suspensões celulares são cultivadas em pequenas gotas invertidas num meio especificamente viscoso e controlado. Forças gravitacionais induzem a formação de esferas de colónias celulares. Alternativamente, culturas envoltas em componentes da matriz extracelular, como matrigel, metilcelulose, fibronectina, laminina e colagénio formam esferoides com características específicas do tumor original. Este tipo de método permite a interação célula-célula e célula-matriz, permitindo inclusive o crescimento e sobrevivência de células dependentes de ancoragem.

Resultados demonstraram que culturas em matrizes com componentes da matriz extracelular, no caso testado em 2.5% (v/v) de matrigel, são fundamentais para a sobrevivência celular de NSCLC, determinando em certos casos uma definida organização estrutural e diferenciação celular.

Métodos para o controlo da viabilidade celular também se encontram disponíveis no mercado, contudo a exata determinação da viabilidade em esferas está limitado à capacidade de penetração dos reagentes indicadores nas mesmas. Propriedades de lise são fundamentais para uma maior sensibilidade, atribuindo as maiores vantagens ao ensaio CellTiter-Glo cujo sinal de fluorescência é proporcional à quantidade de ATP as células.

Resultados demonstram ainda que os níveis de actividade de p-ERK estão especialmente elevados quando as células são cultivadas em 3D, mas que as

demais proteínas envolvidas nas vias de transdução do sinal RAS como p-AKT e p-MLC, não se encontram particularmente alteradas entre os dois métodos de cultura celular.

Diferenças entre 2D e 3D relativamente a dependências do mutante KRAS, foram também estudadas. Primeiramente, um teste com uma biblioteca de 384 inibidores de cinases foi corrido automaticamente em esferas e comparado diretamente com um ensaio independente em 2D para uma linha celular diferente mas com a mesma mutação KRAS. A análise dos dados salientou 10 inibidores como tendo um efeito citotóxico nos esferoides e um efeito oposto de crescimento celular nas culturas 2D. A partir deste ponto novos testes em escala mais pequena foram realizados e novos inibidores, conhecidos por conferir vulnerabilidade às células com a mutação KRAS foram usados. A respetiva viabilidade celular foi monitorizada em 2D e 3D para concentrações crescentes de inibidor.

Dentro da lista de inibidores candidatos usados podem contar-se inibidores das proteínas MEK, PI3K, IKK, PKC, CDK, mTOR, TGF-β, LDH-A, c-Met, Rho e FAK, assim como inibidores do proteassoma e destabilizadores estruturais como a Latrunculina e Paclitaxel. Resultados sugerem que em comparação com culturas 2D, as 3D são especialmente sensíveis a drogas que interferem com a organização da estrutura celular, como é o caso de estabilizadores da tubulina e inibidores da actina. Culturas 3D demonstram também maior sensibilidade perante inibidores da proteína cinase C (PKC) enquanto que culturas 2D são mais vulneráveis a inibidores MEK. Contudo, os resultados indicam ainda que a dependência KRAS é especifica de cada linhagem celular, uma vez que variabilidades entre 2D e 3D podem ser encontradas de caso para caso.

Tentativas preliminares de recriar um modelo *knockdown* especificamente para o mutante KRAS, com RNA de interferência (siRNA), tiveram pouco sucesso. No entanto o desenho deste modelo geneticamente modificado terá significância para futuros testes com culturas 3D. O *knockdown* dum oncogene importante como KRAS torna as células bastante sensíveis. Um modelo estável funcionará como controlo em novos ensaios e determinará a especificidade e atribuição dos resultados à mutação KRAS.

Os resultados alcançados não desvalorizam a importância do uso de plataformas 3D como forma de obter melhores previsões terapêuticas. Pode eventualmente ser a ferramenta indicada para encontrar novos alvos terapêuticos melhorando as perspetivas de tratamento. É porém um trabalho

ainda em progresso que espera novos testes automáticos com largas gamas de inibidores de forma a expor potenciais drogas com exclusiva vulnerabilidade KRAS em culturas 3D.

Palavras-chave: cultura celular 3D; Teste de viabilidade em esferoides; Cancro do pulmão; NSCLC; Inibição da via KRAS; drug screening.

Table of contents

Terminology and Abbreviations

2D - two dimensional

3D - three dimensional

AKT - Protein kinase B

CDK - Cyclin-dependent kinase

CSCs - Cancer stem cells

CTB - CellTiter-Blue

CTG - CellTiter-Glo

DAPI - 4',6-diamidino- 2phenylindole

DMEM - Dulbecco's modified eagle medium

DMSO - Dimethyl sulfoxide

EDTA - Ethylenediamine tetraacetic acid

EGFR - epidermal growth factor receptor

EHS - Engelbreth-Holm-Swarm

EM - Electron microscopy

ERK - extracellular signal regulated kinase

FACS - Fluorescence activated cell sorting

FAK - Focal adhesion kinase

FBS - Fetal bovine serum

FITC - Fluorescein isothiocyanate

GAPs - GTPase activating proteins

GATA$_2$ - Gene encoding for GATA binding protein 2

GEFs - Guanine nucleotide exchange factors

GFP - Green fluorescent protein

H&E - Hematoxylin and eosin

HRAS - Harvey rat sarcoma viral oncogene homolog

ICx - x% of inhibitory concentration

IKK - IκB kinase

KRAS - Kirsten rat sarcoma viral oncogene homolog

LDH-A - Lactate dehydrogenase A

MAPK - Mitogen-activated protein kinase

MEK - Mitogen-activated protein kinase kinase

mTOR - Mammalian target of rapamicyn

NRAS - Neuroblastoma RAS viral (v-ras) oncogene homolog

PBS - Phosphate-buffered saline

PI3K - Phosphatidylinositide 3-kinase

PKC - Protein kinase C

PMSF - phenylmethylsulfonyl fluoride

PVDF - Polyvinylidene difluoride

qPCR - quantitative polimerase chain reaction

RAF - effector of RAS

RAS - Family of GTPases

RB - Retinoblastoma protein

Rho - GTPase

SDS-PAGE - Sodium dodecyl sulfate polyacrylamide gel electrophoresis

SNAIL2 - Tanscriptional repressor

TBST - Tris-Buffered Saline and Tween 20

TCA - Tricarboxylic acid cycle

TEM - Transmission electron microscopy

TGF-β - Transforming growth factor beta

TICs - Tumor initiating cells

Chapter 1

Introduction

1.1- Lung cancer

Lung cancer is a leading cause of death being the most frequent malignant disease worldwide [1].

Only in the Europe, in 2012, around 388.000 people died from this disease [2]. The restricted early detection along with the low therapeutic improvements is considered the major cause for the low survival rate, around 15% [3]. Despite the existence of several efficient drugs approved for the lung cancer treatment, the recurrence after treatment is very frequent, due to the acquisition of resistant point mutations and alternative compensatory pathways beyond the targets of therapy [4], [5].

Thus, the need for the discovery of new targets, allowing the development of new therapies is urgent. Advances in this area will hopefully bring further insights to help clinicians curing patients battling with this disease, providing them a longer lifespan and quality of life.

However, in these days, lung cancer is still a disease with a poor prognosis for patients. Among lung cancer, we can distinguish three types morphologically different: The carcinoids that are neoplasms of neuroendocrine origin [6]; The small cell lung cancer (SCLC), which is less prevalent, is characterized by the microscopic presence of round small cells with limited cytoplasm mostly filled with the nucleus [7]; And the non-small cell lung cancer

(NSCLC), which is the most common type affecting more than 80% of the diagnosed patients with lung cancer. This type is generally subdivided into three main groups comprehending squamous cell carcinoma, adenocarcinoma and large cell carcinoma [8], [9]. The first, being the most frequent, develops from the squamous cells that line the airways and it is often found near the centre of the lung in the bronchus. Adenocarcinoma grows slowly and is arising from the cells that usually secrete substances like mucus and it is found in the outer areas of the lungs. Large cell carcinoma can appear in any part of the lung and tends to grow and spread quickly [10].

Apart from the well known association of lung cancer with smoking, other risk factors arise from a positive family history of the disease. Genetic alterations include, in most of the cases, mutations in the *p53*, *Bcl2*, *Rb*, *FHIT* or $p16^{INK}$ genes. Moreover, telomerase changes, lost of heterozygosity and mutations that activate the *KRAS* oncogene have also been described as risk factors [1], [10].

1.1.1- *RAS* oncogene and signalling pathway

The most prevalent drivers of human cancer are the 3 isoforms of RAS proteins, encoded by *KRAS*, *NRAS* and *HRAS* genes. KRAS activating mutations were described as being the most frequent in cancers [11]. The distribution of mutations for this particular oncogene points out the importance of G12D, the most recurrent mutation [12].

RAS proteins are GTPases that function as molecular switchers of GDP into GTP, playing a key role in the signal transduction involved in the cell survival and proliferation. RAS activation is catalyzed by guanine nucleotide exchange factors (GEFs) to a GTP-RAS state and it is inactivated by GTPase activating proteins (GAPs) to its GDP-RAS state by hydrolysis (Figure 1) [11], [13]–[15].

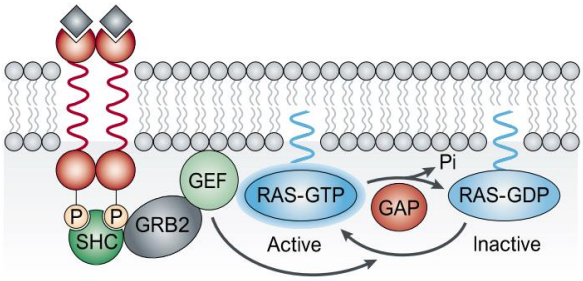

Figure 1. Ras upstream signalling. RAS is activated by GEFs and inactivated by GAPs. When RAS is mutated these interactions are broken compromising the normal cell signalling. (Julian Downward 2002)

KRAS mutations are known to impair GTPase activity blocking the interaction between KRAS and GAPs leading to its constitutive activation [16]. KRAS proteins are thus important players in the cancer development. Its mutation leads to the persistent downstream signalling pathway stimulation, promoting therefore many cancer hallmarks such as uncontrolled cell proliferation, enhanced survival, metabolic reprogramming, cytoskeletal reorganization, increased motility, inflammation and microenvironment remodelling for tumor adaptation [14], [16].

RAS has been described to stand at the top of a bifurcation for a vast network of signalling pathways, targeting several kinases, being the most important ones: RAF, MEK, ERK, AKT and PI3K proteins (Figure 2) [15].

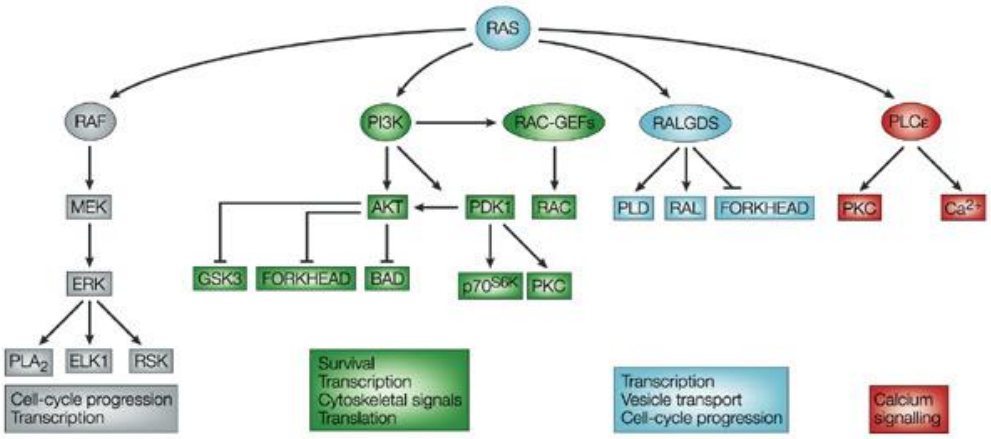

Figure 2. Ras downstream signalling. RAS is involved in the activation of several pathways, controlling several aspects of the cell proliferation, survival and transcription. (Julian Downward 2002) [15].

Although it has been demonstrated that tumor cells with KRAS mutations are dependent on KRAS activity, targeting directly RAS has been demonstrated to be clinically a challenge to date. It is very difficult to design inhibitors for GTPases. Targeting downstream proteins has therefore becoming a focus of attention in the majority of recent studies. Exploiting new possibilities of efficient targets has been constant. Despite the existence of clinically approved inhibitors for downstream effectors of RAS, the ability of RAS to achieve

multiple pathways at different stages has also unveiled the importance of using combined therapies [12], [16], [17].

MAPK pathway, commonly activated in many cancers, leads to RAS activation via adaptor proteins that consequently activate the RAF/MEK/ERK kinase cascade. AKT/PI3K pathway is a parallel pathway that regulates the same functional transcription factors as ERK pathway. Indeed, there are multiple points of crosstalk between these two pathways. They have been described to influence each other at different stages of the signal propagation, determining together the cell fate in a complex and dynamic range of positive and negative loops. This crossed network is a very robust system that shows poor vulnerability to external perturbations [18]–[20].

However, several inhibitory molecules against either MEK or PI3K have been developed with favorable clinic significance and are now under clinical trial. Combination of inhibitory drugs for both targets are also in early-phase clinical trials, with still unclear efficacy and toxicity [21]. Importantly, MEK inhibitors were shown to be selectively toxic for the KRAS mutant genotype whereas PI3K inhibitors did not. Moreover tumors with KRAS mutations were also shown to be selectively dependent on activities that are not directly regulated by RAS. The identification of those factors and pathways that are particularly essential only for cells bearing an activated RAS oncogene, have already been approached with lethal RNA interference screens. The binding kinase 1 (TBK1), the transforming growth factor β–activated kinase 1 (TAK1), the transcription factor GATA2, the CDK4, mitotic regulators and proteasome components appeared as prominent good candidates [21], [22]. Particular dependencies can also be attributed to SNAIL2 in case of the cells that have undergone epithelial mesenchymal transition [23], [24], and MEK, that brings dependencies on RAS mutant cells, along with the insulin-like growth factor receptor (IGF1-R) tyrosine kinase input signal [21].

1.2- 3D cultures

Most of the knowledge brought into light over the past few years has been achieved by pre-clinical cancer therapy research in several cancer cell lines. These cell lines often arise from patient tumors and undergo long term cultivation under specific circumstances. This drags them into a serum-supplied adaptive state, environmentally artificial, known to enhance the accumulation

of genetic alterations. Comparing to *in situ* cells, differences at the molecular level have also been identified, including different expressions in differentiation markers, adhesion and growth factor receptors. Questions come up about the reliability of these models regarding its accuracy in representing the tumors of origin and about its ability to be loyally correlated with clinical predictions [4], [25].

Furthermore, cancer drug development and testing requires relevant cell-based models that can simulate very closely the *in vivo* situation when comes to the point of detecting rapidly the best active drug candidates from large pools of prospective effectors. In this sense, three-dimensional (3D) culture models have been gaining recognition among the scientific community due to its ability to better mimic the *in vivo* conditions, keeping the functional phenotype of tumor cells, and better evaluate therapeutic clinical interventions [26], [27].

3D platforms are valuable tools able to restore morphologic, physiologic, pathologic and functional environmental features of the tumor biology. They bring further insight about tumor organization, homeostasis and cellular differentiation. Moreover, the microenvironment and the surrounding extracellular matrix have been described to play a notorious role into the tumor survival and progression. It also has an impact in the phenotype, gene expression and responsiveness/sensitiveness towards different therapeutic drugs [28]–[30]. Along with these characteristics, 3D cultures are also known to present stronger cell-cell interactions and have a nutrients and oxygen delivery gradient system more similar to *in vivo*. This has thus been contributing to the understanding of altered responses comparing to 2D cultures [26], [27].

In this sense, 3D cultures are promising tools that can improve clinical efficacy predictions, bringing faster results and new anticancer therapeutic strategies. It may also reduce experimental costs, avoid unnecessary preliminary trials and replace some animal tests, which is undoubtedly a step forward for the researchers and pharmaceutical industry [31], [32].

1.2.1- 3D culture systems

Currently there are several 3D *in vitro* culture methods. Not all of them work for all the cell lines and some require very specific instruments, being hardly reproducible. Among others, 3D cultures include shaking-based approaches, non-adherent round surfaces, microfluidic systems, hanging-drop techniques, scaffold-based models, cell printing and matrix embedding. The

latter uses extracellular matrix proteins like matrigel, methylcellulose, fibronectin, laminin and collagen.

Suspension methods as non-adherent surfaces on repulsing substrates and hanging-drop techniques generate simple aggregates of cells. Hanging-drops are drops of cells in suspension which are then inverted. The specific viscosity of the media within which they are seeded determines the right properties for its hanged sustention. In this case, gravitational-enforced cell settling and cell-cell adhesion leads to the self-assemble of spherical clusters of cell colonies (Figure 3) [32].

Alternatively, matrix embedding techniques allow the formation of spheroids with tumor specific features. This sort of methods overcome the lack of cell-surface adhesion of the traditional 3D cultures, which are very often known to impair cell survival of anchorage dependent cells. Matrix embedded cells have both cell-cell and cell-matrix attachments. When proteins from the extracellular matrix are incorporated in the culture medium, tissues structure and some of their differentiated functions are preserved (Figure 3). Matrigel is one of the most commonly used materials to construct 3D models. It is a basement membrane preparation extracted from the EHS mouse sarcoma that is rich in extracellular matrix proteins, including laminin, collagen IV and entactin. Altogether they form an organized structure able to sustain cell growth and survival [32], [33].

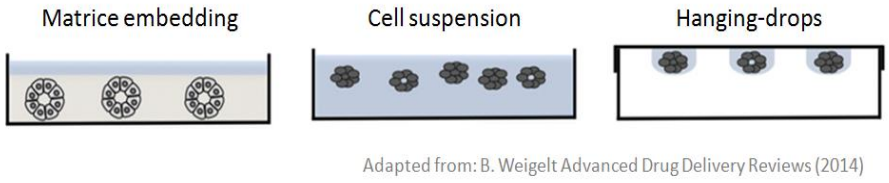

Figure 3. 3D culture systems. Matrice embedding maintains structural and functional properties of tumor cells. Cell suspension and hanging-drops form spontaneous agglomerates of cells.

Additionally, once the sustained proliferation is a characteristic of tumor cells, all 3D models must allow the monitoring of cell viability. Plus, most of the results from drug assays are mainly based on the survival of cells, reinforcing the importance of gather 3D models with an accurate viability test.

There exist viability tests based on the metabolic activity of cells, the presence of ATP or other redox metabolites. Cells' ability to metabolize and react with certain products are afterwards detected mostly by spectroscopy and correctly quantified, being the results correlated with the amount of live cells. Other methods are based on investigating cells' integrity or the presence of certain molecules or markers well known to trigger apoptosis [34].

1.3- 2D *vs* 3D differences

Bearing in mind the advantages of 3D culture models, efforts to recreate this kind of platforms with NSCLC cells appear to be a new priority. Such efforts will definitely bring more reliable results either on drug screens or in the understanding of simple signalling pathways.

In this sense, comparing 2D and 3D cultures is essential to understand whether it can convey major differences that may underestimate 2D culture experiments.

Specifically, understanding how dependent RAS pathway is from the culture method and how different the already observed characteristics of mutant KRAS cell lines are from the culture system, can surely bring new insights and perhaps, change the way assays should be done in order to get closer approaches to the *in vivo* situation.

Comparisons involve then morphologic features, signalling pathway aspects and examination of the different sensitivities and vulnerabilities towards drug treatments.

1.3.1- Targeting KRAS effectors

As has already been described before, Julian Downward's lab has investigated unique dependencies of RAS mutant cancer cells over the past years, highlighting a number of vulnerabilities of RAS mutant cells [21], [22]. One term of comparison between 2D and 3D cultures was therefore the use of a selection of effectors that have already been demonstrated to be essential for the survival of KRAS mutant cells.

The urgent need to test several of these established effective inhibitors on 3D cultures in an attempt to find divergences that would eventually refute previous results made in 2D cultures was subject of study for NSCLC cell lines.

1.3.1.1- Candidate inhibitors

In order to compare KRAS dependencies in 2D and 3D settings, several inhibitors were tested. That includes drugs targeting KRAS downstream effectors or other pathways that have been demonstrated to be important for the survival of cells harboring KRAS mutations [15].

- MEK inhibitors - Permanent active forms of MEK are implicated in the development of several human cancers [35]. Targeting the mitogen activated protein kinase (MAPK) pathway with highly selective inhibitors of MEK has been proved to inhibit efficiently ERK activation. Therefore blocking proliferation, survival and motility of *in vitro* tumor cell lines under certain circumstances. It has also been proved to be effective on the growth inhibition of tumors in immunodeficient mice [15], [36].

- PI3K inhibitors - KRAS mutations also lead to growth stimulation through AKT activation, because of the crosstalk between ERK and PI3K/AKT activation. Consequently, regulation of each other determines the efficacy of MEK inhibitors [3], [18]. Breaking down this ERK/PI3K interaction seems then to be a good target, as was already observed *in vivo* assays [16], [37].

- Proteasome inhibitors - Along with the previous kinase inhibitors (MEK and PI3K inhibitors), there is also a clear need to interfere with the largely studied kinase/protease crosstalk, which can be achieved by proteasome inhibition. Many kinases are regulated by proteolytic cleavage and in turn, many other proteases activity can be switched on or off by phosphorylation [38].

- IKK inhibitors - NF-kB proteins are transcription factors that have been described as having an important role in inflammatory diseases. Abnormal

regulation of these proteins can lead to autoimmune diseases and several types of cancer. Regulation of NF-kB is carried out in part by IKK. Moreover, IKK-β activity is required for protection from apoptosis. Efforts to inhibit IKK have then been matter of interest. IKK inhibition has also been proven to be effective in reducing lung cancer cell proliferation *in vitro* and blocking tumor growth *in vivo* especially for patients with *KRAS* mutation [17], [39].

- PKC inhibitors - Protein kinase C family regulates a diverse set of cell processes such as cell survival, proliferation, migration and apoptosis, being ultimately involved in malignant transformation when cooperating with RAS. Different isozymes are responsible for the activation of AKT and ERK, increasing anchorage-independent growth, metastasis and tumorigenicity. Its inhibition was then a target for the NSCLC cells 3D models [40], [41].

- CDK inhibitors - Cyclin-dependent kinases are important cell-cycle regulators. CDK4/CDK6 are activated by cyclin D1, which in turn is regulated by many signalling intermediates including RAS-MEK-ERK and PI3K-AKT pathways. Increased activation of cyclin D1-CDK4/CDK6 leads to the phosphorylation of RB (retinoblastoma protein), which induces the transcription of E2F-responsive genes increasing proliferation. Therefore, abrogation of CDKs activity is thought to be an effective therapeutic approach [42].

- mTOR inhibitors - mTOR is activated by PI3K, an effector of RAS pathway, which in turn is able to activate AKT and consequently the downstream pathway contributing to proliferation and cell survival. Its inhibition *in vitro* and *in vivo* pre-clinical models has been shown to inhibit proliferation [43].

- TGF-β inhibitors - In cancer cells, the MAPK upstream TGF-β regulator has been seen to be activated simultaneously with RAS-MAPK, acting synergistically in tumorigenesis [44], [45].

- LDH-A inhibitors - Chemical compounds such as lactate dehydrogenase A (LDH-A) inhibitors, were seen to decrease tumorigenesis in NSCLC driven

by KRAS or EGFR oncogenes. Researchers have also seen that abrogation of LDH-A in tumors that rely on hypoxic niches reduces the Warburg effect in NSCLC *in vivo* and *ex vivo*. However reactivation of the TCA cycle happens *in vitro* reinforcing the microenvironment importance in the tumor metabolic reprogramming and consequent cells survival [5].

- c-Met inhibitors - Literature has recently shown a Met indispensable dependency for anchorage-independent cell growth on KRAS mutants [46].

- Rho inhibitors - Rho GTPases are a family of RAS oncogenes that promote signal transduction upon binding to GTP, controlling cell morphology and actin cytoskeleton. Its inhibition would then attenuate the constitutive effectors from generating a cellular response. However the spatiotemporal control of Rho-GTPases might restrict its activity [47]–[49].

- FAK inhibitors - The nonreceptor Focal Adhesion Kinase (FAK) can bind an activate signalling proteins such as PI3-K, many times activated in KRAS mutant cancer. Its inhibition has also been identified as a promising anti-tumorigenic agent [20], [50].

- Latrunculin and Paclitaxel - Other approaches may also be effective when interfering with the structural organization of the spheres, or hamper its morphologic stability. In theory this strategy might bring little or no major harm to monolayer cells, that do not present a well defined structural multicellular organization, while in 3D cultures it should already been taken in consideration. In this same way, cytoskeleton interfering drugs such as Paclitaxel and Latrunculin appear to be worth trying and analyzed between both, 2D and 3D culture systems.

1.3.2- KRAS knockdown

Despite the efforts, the direct inhibition of KRAS is still not possible. However advances in selectively knocking down the oncogenic KRAS is known to be therapeutically effective and to suppress tumor growth in NSCLC.

Although, in certain cases targeting KRAS by itself might not be sufficient but leastwise it sensitizes tumor cells, opening possibilities of combining this strategy with other target therapies [14], [51].

The use of small interfering RNA (siRNA) in spheroid cultures, in order to genetically manipulate the expression of an important oncogene like KRAS is valuable. Cells are very sensitive to its knockdown and effects on cell viability are already known. A stable model can work as a control for drug assays, showing specific and unique KRAS dependencies and vulnerabilities.

1.4- Aim of the work

3D culture models are known to better predict therapeutic outcomes due to its ability to better simulate the *in vivo* morphologic, physiologic, pathologic and functional environmental features of the tumor biology. Targeted anticancer therapies with 3D tools are still barely explored and further insights into this field would definitely benefit *in vivo* treatments. Based on that, the aim of this study is:

- To set up a method that allow the survival and growth of RAS mutant lung cancer cells in 3D cultures;

- To identify an accurate method to monitor cell viability in 3D cultures, suitable for large-scale screening;

- To compare the dependencies of RAS mutant cells and drug vulnerabilities in 2D and 3D cultures.

Chapter **2**

Materials and Methods

The aim of this work was to develop a three-dimensional culture method that would allow the survival and growth of KRAS mutant cell lines. The purpose of this methodology is to guarantee a closer approach to the *in vivo* situation of non-small cell lung cancer, providing a more effective tool to test clinical antitumor drugs.

2.1- 3D culture methods

NSCLC cell lines were previously generated in the lab and were obtained from KRAS mutant alone and KRAS mutant plus p53 deleted mice lung tumors and metastasis. All cell lines were initially grown in monolayer at 37ºC in 5% CO_2 with normal media: Dulbecco's Modified Eagle's Medium (DMEM) with 10% (v/v) fetal bovine serum (FBS), 1% (v/v) glutamine and 1% (v/v) penicillin-streptomycin antibiotic.

2.1.1- Soft agar

6 well plates were initially coated with equal volumes of 1.2% (w/v) agarose at 42ºC in distilled water and 2x normal media to give 0.6% (w/v) agarose in 1x media.

Cells were previously washed in Phosphate-buffered saline (PBS) and trypsinized with 1x trypsin solution. After its collection with normal media and centrifugation at 1200rpm for 4min, the pellet was re-suspended in normal media and filtered through a standard FACS filter (70µm pore size) to guarantee that cells would be plate as single cells.

Cells were counted and 40000 cells were then plated in triplicate with 0.3% (w/v) agarose in 1x media at 42ºC over the previous base layer.

After set down, normal media was dropped onto surface and repeated every 3 days during 3weeks. Cells were kept on 37ºC in 5% CO_2.

2.1.1.1- Giemsa staining

After 3 weeks on culture, colonies from soft agar cultures have been stained with Giemsa, a modified solution Fluka 48900: 1 part Giemsa + 5 parts glycerol:methanol (5:24 parts).

Media was removed from agarose surface and 1mL of Giemsa was added and kept 20min under gentle agitation. Afterwards, several washes were carried out with water under gentle agitation, including one wash overnight.

2.1.2- Non-adherent round bottom plates

Trypsinized cells were centrifuged, re-suspended and filtered to avoid agglomerates.

Triplicates of 5000 cells were then platted, in Corning® 96 Well Clear Round Bottom Ultra Low Attachment Microplates, either with normal media or with media without FBS, followed by incubation at 37ºC in 5% CO_2. Cells were kept in culture for 7 days with regular feeding.

2.1.3- Non-adherent coated plates

Flat bottom Corning® 96 Well plates were coated before the seeding of 5000 cells per well.

2.1.3.1- Agar coating

Plates were coated with the same base layer used on soft agar protocol. 50µl of 0.6% (w/v) agarose (at 42ºC) in 1x normal media was added to each well and set down.

2.1.3.2- Polyhema coating

Poly(2-hydroxyethyl methacrylate) was dissolved with ethanol in a hot water bath with stirring to a final concentration of 0.12g/ml (10x). The solution was filtered to remove impurities in a sterile syringe filter with 0,2µm pore size. 100µl of a 10 times diluted solution was added to each well and evaporation happened upon incubation of the plate at 65ºC. The process was repeated once more before loading cells.

2.1.4- Hanging drops

There are available on the market a set of plates that allow to perform this technique easily, however it was made inverting normal 10cm dishes.

A 1.25% (w/v) methylcellulose stock solution was pre-made in normal media, corresponding to 5x of the desired final concentration, which is 0.25% (w/v) methylcellulose. The solution was then diluted to 2x with normal media and filtered with a 0,44µm pore size syringe filter to remove impurities.

Cells were trypsinized and after centrifugation at 1200rpm for 4min, the pellet was re-suspended and filtered through a standard FACS tube to avoid agglomerates. Cells were then counted and a stock cells solution made with the amount of desire loaded cells per 10µl of normal media. Equal volume of 2x methylcellulose was afterwards pipetted to the stock cells solution and drops of 20µl plated in triplicate into the lid of a 10cm petri dish (Figure 4).

Ex.: For 10 drops with 5000 cells each, around 110µl with 55000 cells will make the stock cells solution. Then 110µl of 2x methylcellulose is added giving a final solution of 220µl of 0.25% (w/v) methylcellulose with 55000 cells. In this way, each 20µl drop will have 5000 cells.

Distilled water was added to the bottom of the petri dish to form a wet chamber and the lid inverted towards the top of the dish. Drops were then kept at 37°C in 5% CO_2 overnight.

On the following day, spheres should have been formed and can easily be seen by eye. Each sphere was then carefully pipetted into individual 96 flat well plates, pre-coated with 0.6% (w/v) agar, and finally filled with 100µl of normal media before returning to the incubator at 37°C in 5% CO_2.

At this stage, cells can be kept in culture for more than one week and regular feeding with 25µl of normal media was ensured every 3 days.

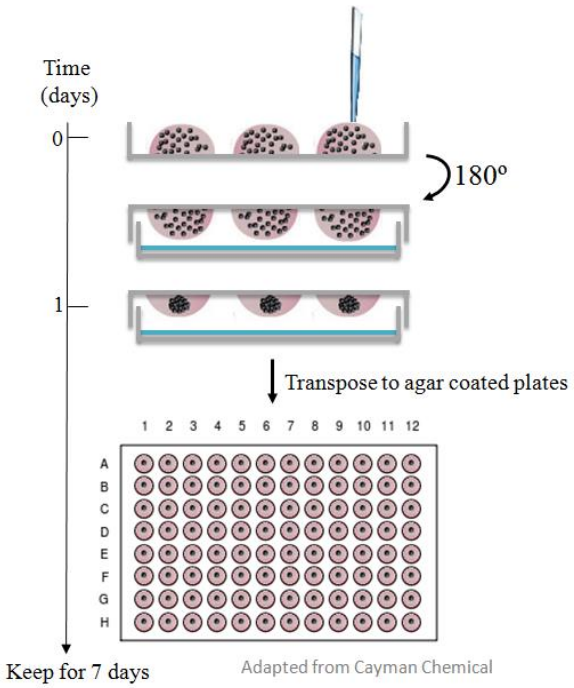

Figure 4. Hanging drop technique illustration. 20µl of cells in 0.25% (w/v) methylcellulose are hanged on a lid that is inverted into a wet chamber. Overnight incubation under gravitational forces allows the cohesion of cells into spheres that can be transposed on top of agar coated surfaces, where they can remain alive for more than one week.

2.1.5- Matrice embedding

2.1.5.1- Matrigel

For this procedure Matrigel® matrix basement membrane with growth factor reduced was supplied by Corning®. It was perform on ice and all used materials were properly pre-cooled at 4°C to avoid matrigel solidification.

Cells in 2D cultures (10cm plates) were washed in PBS and trypsinized.

Cells were collected with normal media (10% (v/v) FBS) to a falcon tube and centrifuged for 4min at 1200rpm.

The supernatant was discarded and the pellet was re-suspend in normal media. It was filtered through a standard FACS tube (70µm pore size) to remove potential clumps.

Cells were then counted and diluted to have 2x the amount of cells to be plated (solution A). Ex.: For 96 wells with 2500 cells per sphere/well, solution A have around 265.000 cells in 5.3ml.

On ice a 2x matrigel solution was made in normal media (solution B). Matrigel was gradually dissolved, pipetting up and down, with little cold amounts of normal media in order to achieve an homogenous solution.

On ice, solutions A and B were mixed together in a 1:1 proportion.

On ice, the cell-matrigel mixture was poured into disposable reservoir liners and with a multichannel pipet, 100µL of the content was pipetted into the wells.

Afterwards, the plate was centrifuged at 1000 rpm at 4°C during 15-20secs. Plates were then kept at 37°C in 5% CO_2.

48h later a compact sphere should have been formed. Spheres can be kept in culture for more than one week with every three days feedings with 25µl of normal media.

2.1.5.2- Methylcellulose

This procedure follows the main guides from the matrigel embedding spheres protocol described above, but it is carried out at room temperature.

A 1.25% (w/v) methylcellulose stock solution (5x) was pre-made in normal media. Before being used it is diluted with normal media into 2x and properly filtered with a 0,44µm pore size syringe filter to remove impurities.

2.2- Viability methods

2.2.1- CellTiter-Blue assay

This is a light sensitive end-point assay. Direct light sources were avoided during all the procedure.

5µl of CellTiter-Blue was added to each well of 3D or 2D cultures including the respective blanks and incubated at 37ºC for 2h. In this period viable cells were able to convert by reduction resazurin to the fluorescent resorufin product (Figure 5). Plates were then read in the PHERASTAR Plus microplate reader, set up to read the fluorescence emition signal at 590nm.

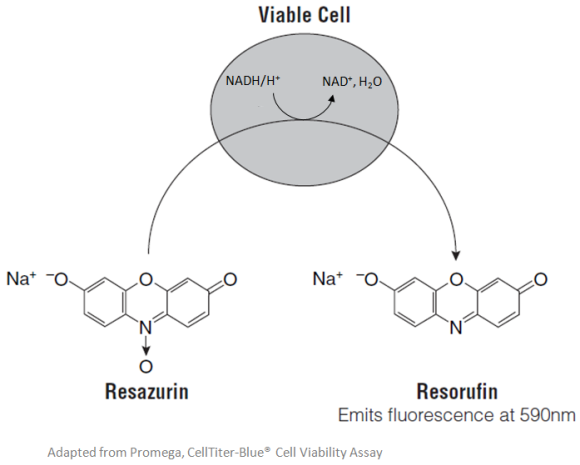

Figure 5. Redution of resazurin in resorufin. Fluorescence signal should be proportional to the number of metabolically active cells.

2.2.2- CellTiter-Blue with EDTA treatment

In this end-point viability assay for 3D cultures, 10µl from a 50mM EDTA solution was added to each well, having as final EDTA concentration 5mM. Plates were briefly stirred and incubated at 37ºC for 45min to allow spheres disruption. Therefore, 5µl of CTB was added to the wells followed by 2h incubation and 590nm fluorescence reading with the PHERASTAR Plus microplate reader.

2.2.3- Tryphan blue staining

The use of this method is wide spread in 2D cultures for routine cell culture counting. To be used in 3D cultures, spheres were first disrupted with 5mM EDTA (final concentration) at 37ºC for 45min. Next, 10µl of the sample was mixed with 10µl of tryphan blue and pipetted into a cell counting slide. It was then inserted in a cell counting instrument and the concentration of live cells was automatically displayed.

2.2.4- Integrated density of the GFP fluorescence

The determination of the intensity fluorescent signal of spheres from microscopic images was done with ImageJ software.

First, images were treated with the same software to delineate the spheres perimeter. To do so, threshold was established and particles above the defined size identified and individually selected. In this way the same mask could be used for the original FITC image (corresponding to the sphere GFP signal). Afterwards measurements were done taking in account the blank that correspond to the black coloured area of the image (Figure 6).

Hereby, one of the set measurements given was the integrated density, with which further analysis were made.

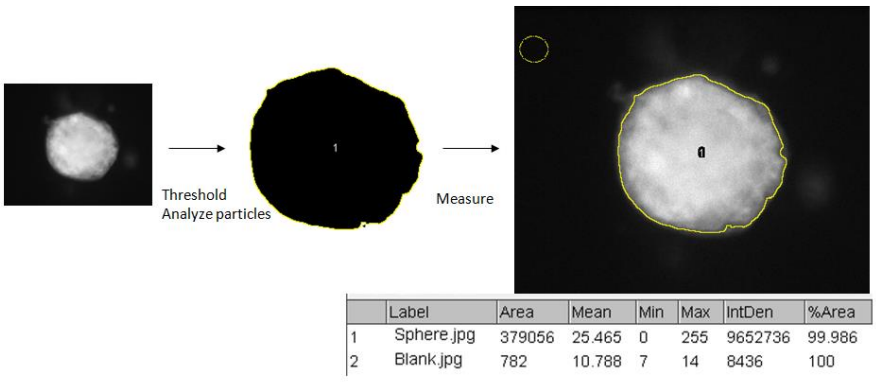

	Label	Area	Mean	Min	Max	IntDen	%Area
1	Sphere.jpg	379056	25.465	0	255	9652736	99.986
2	Blank.jpg	782	10.788	7	14	8436	100

Figure 6. Measuring spheres fluorescence using ImageJ. Several steps were executed in order to get the integrated density signal of each sphere.

2.2.5- Acumen - GFP fluorescence signal

The area of GFP positive cells could be automatically determined with the Acumen Explorer eX3 laser scanning microplate cytometer (TTPLabtech), allowing the size monitorization of spheres through time.

2.2.6- CellTiter-Glo assay

CellTiter-Glo® Luminescent Cell Viability assay was a product supplied by Promega.

This is a temperature dependent and light sensitive assay. In this way, spheres were left at room temperature for 30min along with the CellTiter-Glo reagent to stabilize.

After that, 50µl of reagent was added to each well, followed by 2min of vigorous shaker agitation and 15min stabilization. Plates were kept away from direct light sources every time possible.

Cells are then lysed and ATP is released, allowing a luciferase catalyzed reaction to take place. In the presence of ATP, Mg^{2+} and O_2, luciferin is converted into the oxyluciferin fluorescent product by mono-oxygenation (Figure 7).

Plates were then read in the PHERASTAR Plus microplate reader, with the correct settings for luminescence.

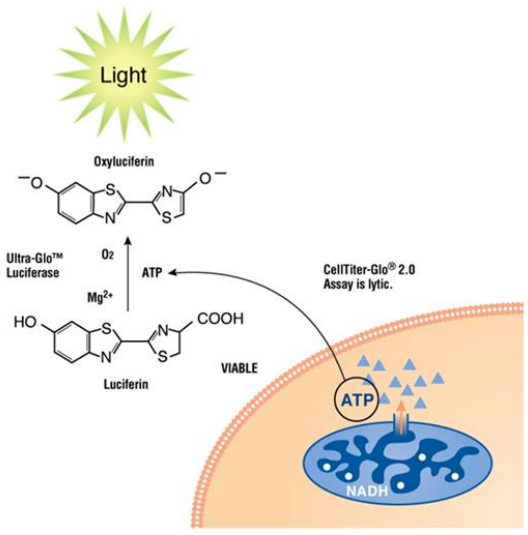

Adapted from Promega, CellTiter-Glo® 2.0: A Luminescent Cell Viability Assay

Figure 7. Conversion of luciferin into oxyluciferin. This mono-oxygenation reaction is just carried out in the presence of ATP that is released by lysed live cells. The signal is thereby proportional to the number of live cells.

2.3- Morphology of spheres

2.3.1- TEM and EM

Images of the spheres by Transmission electron microscopy (TEM) and Electron microscopy (EM) was a part of the project performed by the Electron Microscopy facility of the Francis Crick Institute. They provided the equipment and expertise necessary to get high resolution images.

Spheres were cultured under the desired conditions, 2.5% (v/v) matrigel, and plates were taken to the Electron Microscopy facility which took care of the following steps until image acquisition.

2.3.2- H&E and E-cadherin staining

These assays were carried out by the Experimental Histopathology facility of the Francis Crick Institute.

Spheres were cultured for one week in 2.5% (v/v) matrigel. The following procedures for Hematoxylin and eosin stain (H&E) and E-cadherin staining were elaborated by the facility which provided the final images.

2.4- Western blotting

2.4.1- Protein extraction

Cell lysis buffer supplied by Cell Signaling was used for protein extraction. This 1% triton lysis buffer was prepared being previously diluted to 1x with distilled water. 25mM of NaF and 1mM of PMSF (dissolved in ethanol)

as final concentrations were also added, along with 10% (v/v) of protease inhibitors and 1% (v/v) of the phosphatase inhibitor cocktail.

For protein extraction on 2D cells, 24 wells from the 96 well plates were used for the same conditions. 2D cells were washed twice with cold PBS, scraped and solubilized in cell lysis buffer. The samples were kept on ice during 20min for better lysis. Eppendorfs were then centrifuged at 4ºC for 10min at 13000rpm and the pellet discarded. Samples were kept at -20ºC until blotting.

3D protein extraction required 48 spheres with 10000 cells each for each condition. 3D cells were carefully taken from the plate and transferred to an eppendorf where they were washed three times with cold PBS to dilute the matrigel and remove FBS. Cells were then solubilized with cell lysis buffer and kept on ice for 1h pipetting up and down every 15min to disrupt spheres. They were then centrifuged at 4ºC for 10min at 13000rpm and the pellet discarded. Samples were kept at -20ºC until blotting.

2.4.2- Blotting

Protein concentration of the aliquots with cell lysates was quantified with the bradford assay. Samples were then prepared to load into gels with 1x Laemly buffer plus 10% (v/v) β-mercaptoethanol. The low amount of extracted protein from the spheres just allowed to load 2µg of protein.

Aliquots were sonicated for 10sec, boiled 5min and subject of SDS-PAGE. Proteins were then transferred to PVDF membranes and immunoblotted with different antibodies.

For chemioluminescent detection, 5% (v/v) BSA in TBST-0.05% (v/v) (Tris-Buffered Saline and Tween 20) was used to block the membranes against nonspecific epitopes. Whereas for the LI-COR system, which is an infrared fluorescent detection method, the especific Odyssey® Blocking Buffer was used.

Primary antibodies were prepared in the corresponding blocking solutions in a concentration of 1:2000, apart from the p-Akt(T308) and p-Akt(S473) which concentration was 1:750. Secondary antibodies were prepared as 1:5000 in blocking buffer. Vinculin is a housekeeping protein used as loading control. All washes were made with TBST-0.05% (v/v).

Re-probing membranes entailed the use of stripping buffer.

Variations in protein expression levels were quantified with ImageJ software using densiometry values.

2.5- Preliminary drug screen

Drug screen was performed by the High Throughput Screening facility of the Francis Crick Institute that was provided with the desired 3D cells, in this case MetA cell line.

Cells were monitored with the acumen, as already described above, and spheres' area measured before treatments and at 24h, 48h, 72h and 6 days after treatment with a kinase library drug screen for 384 wells. Single spheres treatment was applied and no replicates were used. Every drug was used with a standard concentration of 10μM.

2.5.1- Determination of hit drugs

Comparisons were made between 3D cultures of MetA line and 2D cultures from other cell line of a previous kinase library drug screen.

First the fold change size of DMSO control spheres were measured comparing the day 6 of treatment with pre-treated spheres. A median of 424% fold change was found with a standard deviation of 107%. These values were taken into account to classify the drug effect on treated spheres. In this sense, 6 days after treatment, drugs that produced a spheres' fold change of 317-531% were classified as cytostatic drugs, with null effect. Drugs that lead to fold changes between -100% (minimum value) and 107% were considered cytotoxic. Finally, fold changes above 531% categorized the drug as having a positive growth effect.

A drug cytotoxic effect was then search for 3D cultures. Taking in account the found drugs, a simultaneous cytostatic or growth effect was tracked for the available screen on 2D cultures. In this case, cells' confluence was measured and drugs with values above 10 were assumed to have enhanced cell growth.

Thereby, 10 different inhibitors were selected and subject of further analysis.

2.6- Drug assays

For all drug assays, 2500 cells in 2.5% (v/v) matrigel were used for 3D cultures and 1000 cells were used for 2D cultures. 50µl of the desired diluted drugs were added in a 3x concentration upon 48h to each well of the 96 well plates. Viability assays were performed for all samples upon 72h of treatments.

Drug treatments for protein extraction required shorter incubation periods and final drug concentration met the correspondent IC_{30}.

2.6.1- Dose curve and IC_{50}

Dose curves were based on the viability of cells, either on 2D or 3D cultures, upon 72h of drug treatments with gradual dilutions. CellTiter-Blue was used to measure 2D viability, whereas CellTiter-Glo was the preferred method for 3D cultures.

The percentage of viability was calculated against the DMSO control and values plotted on a graph with GraphPad Prism software. A non-linear regression with an equation for dose inhibitory response with four parameters was then drawn and the IC_{50} was determined with the displayed curve values.

2.7- MEK inhibition resistance

3D cultures of LKR and D lines were treated for 10 days with a correspondent IC_{70} dose of the MEK inhibitor Trametinib. 50µl of Trametinib was added new every 3 days.

Trametinib survival cells were trypsinized and transferred to monolayer into 10cm petri dishes. Afterwards, cells were assayed again for Trametinib response in 2D and 3D cultures and IC_{50} determined as described in the previous subsection.

2.8- KRAS knockdown spheres

For all experiments cells were plated in the absence of antibiotics and usually cells were starved the day before with no serum.

siRNA was performed in 3 different ways:

1- Transfection took place at the same time as cells were plated into 3D cultures:

In this assay 2500 cells were used in 2.5% (v/v) matrigel. Oligonucleotides (siRNA KRAS pool, RISC-free and scramble) were used at 25nM as final concentration and DharmaFECT™ transfection reagent supplied by Dharmacon ™ was used.

To do so, for each well, 2x solutions were made. 1µl of 5µM oligonucleotides was added to 9µl of DMEM and 0.4µl of DharmaFECT reagent was added to 9.6µl of DMEM. Both solutions were mixed and incubated for 20min at room temperature. Then 80µl of antibiotic-free normal media were added to a final volume of 100µl (solution A).

The preparation of cells in matrigel was also made with 2x concentrations. Thereby, for each well, 25ul with 2500 cells were mixed with 25µl of 10% (v/v) matrigel.

Finally, equal volumes of solution A and cells were mixed, plated and centrifuged (as described in section 2.1.5.1) to give 2500 cells in 2.5% (v/v) matrigel transfected with 25nM of oligonucleotides.

2- Transfection was made 2 days after platting cells into spheres:

In this case, 3D cells in 2.5% (v/v) matrigel were transfected with oligonucleotides for a final concentration of 125nM. 5µM siRNA stock solution and DharmaFECT reagent were used. Spheres were carefully washed with cold PBS to remove matrigel before transfected with 100µl.

3- Transfection was done in 2D cultures.

For this assay, 15000 cells were plated in 6 well plates for two days. Low confluence cells (30-50%) were transfected with Oligofectamine™ reagent supplied by Invitrogen™ with 200nM of oligonucleotides as final concentration.

To do so, for each well, 4µl of Oligofectamine reagent was diluted with 11µl of DMEM and incubated for 10min at room temperature. Then, 40µl of 5µM stock oligonucleotides were diluted with 145µl of DMEM, mixed and incubated with the previous solution for 20min at room temperature. Finally 800µl of DMEM was added to the mixture and 1ml was poured into the cells. After 4h of incubation at 37ºC in 5% CO_2, normal media with 3x FBS was added.

On the following day 2D transfected cells were transferred into 3D cultures as described in the procedure of section 2.1.5.1.

Lysates were collected after transfection from 2D and 3D cultures to confirm the efficiency of the procedure by qPCR.

Cells were monitored after 48h for viability with CTB assay.

2.9- Data analysis

Data was in part analysed with Microsoft excel to determinate triplicate average, standard deviation, to subtract blank, calculate fold changes and viability percentages as well as to calculate new standard deviations accordingly to the analysis made.

Worked data was then plotted with GraphPad Prism which allowed the determination of several parameters.

Chapter **3**

Results and Discussion

3.1- Design of a 3D culture method

The first aim of this project was to develop a method that will allow the growth and survival of lung cancer cell lines into 3 dimensional conditions. For that purpose, seven different established cell lines of non-small cell lung cancer cells were used. Six of them are established from NSCLC tumors with KRAS mutant and p53 deleted ($KRAS^{G12D/+}$; $Trp53^{F/F}$; $Rosa26^{mTmG/+}$ mouse model): B, D, F, E, MetA and MetB lines; the latter two coming from a metastatic site. The seventh cell line is LKR line that has been established from NSCLC with KRAS mutant but wild-type p53 ($KRAS^{G12D/+}$; $Rosa26^{mTmG/+}$ mouse model). Additionally, all cell lines express the green fluorescent protein (GFP) apart from LKR.

3.1.1- Soft agar cultures

At the first place, a simple and fast method was used to check which cells would have a positive growth under non-anchorage independent conditions.

As described in the materials and methods section, cells were kept in soft agar plates for three weeks, generating agglomerates in only four cell lines: LKR, D, E and MetA lines (Figure 8). Sphere formation in these specific cell lines points for the existence of a bigger population of cancer stem cells (CSCs)

or tumour-initiating cells (TICs), which has been identified as a property of CSCs [4], [27].

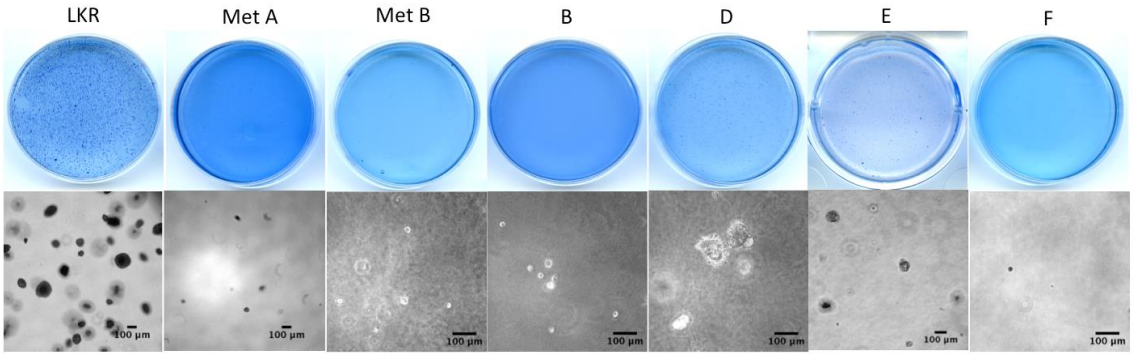

Figure 8. Non-anchorage independent cell growth is observed for certain NSCLC cell lines. End-point assay of soft agar cultures with 40000cells. Giemsa staining, on the upper panel, shows the formation of colonies after three weeks for LKR, MetA, D and E lines. The lower panel shows microscopic images of the corresponding soft agar plates.

This method has allowed us to identify LKR, D, E and MetA lines for future experiments. However, the use of this method is not ideal for automation and high-throughput screenings with drugs, explaining the further search for different non-adherent growth methods.

3.1.2- Non-adherent surfaces

3.1.2.1- Non-adherent round bottom plates

Taking in account the previous results the following step was to test non-adherent round surfaces with the cells that had grown in soft agar. This is an easy and straightforward method known to allow cell growth in suspension. Moreover, as had already been described before, the absence of serum had a positive impact on cell growth, which was also tested [27].

The metastatic cell line MetB is used here as a negative control for the anchorage-independent growth. After one week, MetB does not form spheres when plated without serum. It appears with a scattered morphology composed

by some small agglomerates and some cells attached to the bottom of the plate. On the other hand, D and LKR lines, both in starvation and normal media conditions, showed a decrease in the diameter of the overall sphere. Moreover, the morphology indicates that the cells are fused together, but with an unhealthy appearance (Figure 9). Thus, although the use of non-adherent round bottom plates is an easy and fast method, it is not useful for our purposes.

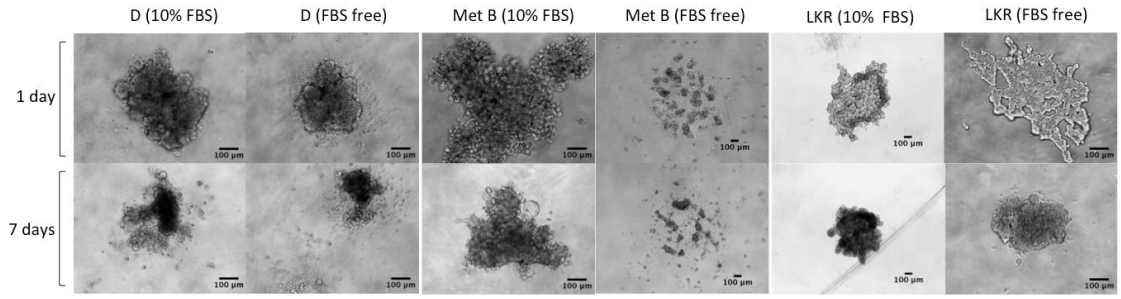

Figure 9. Cells form clumps and shrunk in non-adherent round bottom plates. D and LKR lines were cultured in the presence and absence of FBS serum in non-adherent round bottom plates, being monitored through 7 days. Microscopic images show a clear shrinking and unhealthy morphology upon 7 days. The negative control, MetB line which does not grow in soft agar, shown to be able to attach the plate and does not form clumps.

3.1.2.2- Non-adherent coated plates

Once the last results did not show satisfactory cell morphology after one week culturing, other simple methods were tested. The use of coated plates has already been described by several laboratories. Cells were seeded as stated above in material and methods on top of either 0.6% (w/v) agar or polyhema and followed for one week.

In both coatings cell growth was observed, and cells have a similar morphology to the negative control, line B. Agar 0.6% (w/v) allowed cells to form quite lose agglomerates which got more condensed over time. On the other hand, polyhema coated surfaces, shows a randomly formed tubular shape that seems to have packed together after one week for B and LKR cell lines (Figure 10).

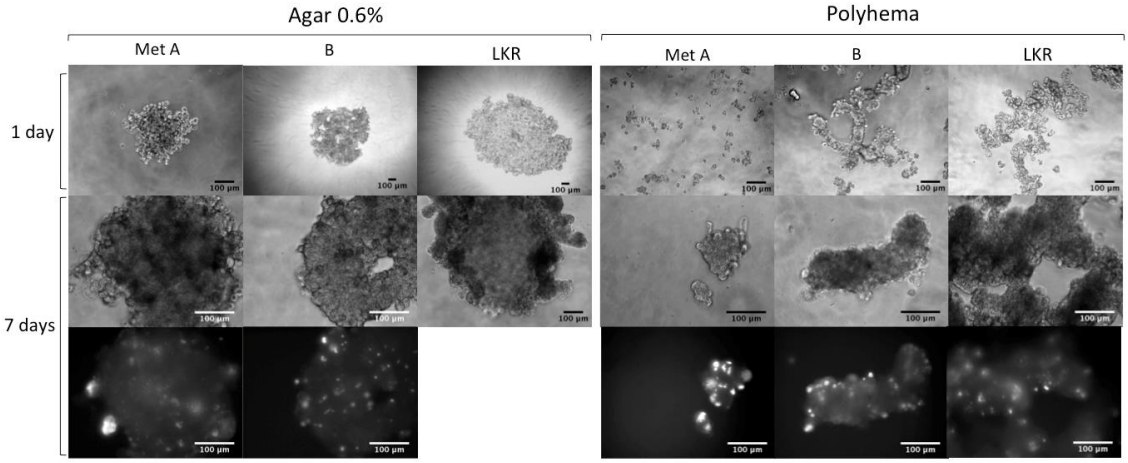

Figure 10. Cells form clumps and appear with high levels of DAPI foci in non-adherent coated plates. MetA, B and LKR lines were kept in culture for 7 days in coated plates, either agar 0.6% (w/v) or polyhema. Microscopic images along with DAPI staining after 7 days (bottom row) indicates high levels of cell death.

For both coating systems, DAPI staining indicates that the amount of dead cells is significantly high, proven some degree of toxicity of these coating surfaces.

3.1.3- Hanging drops technique

The hanging drop technique, as described in materials and methods, is used by many research groups with satisfactory cell growth results [52]. Tests with this method showed certain handling difficulties inappropriate for automated screens. However, culturing cells on an hanging drop appears to have an important role in the cohesion of cells and in shaping a sphere that remains intact for at least 7 days after transference into an agar coated well.

In overall, spheres shrink over time, appear darker and more compacted with an apparently more organized structural morphology (Figure 11).

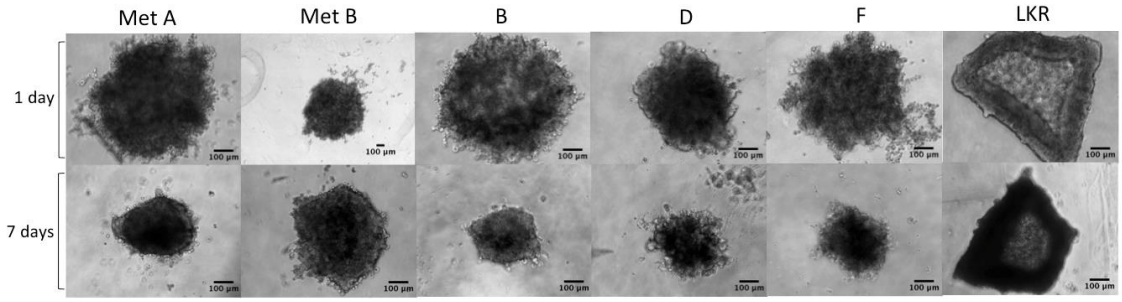

Figure 11. Culturing cells in hanging drops allows its shaping and cohesion. Microscopic images of cells on top of agar after had been shaped overnight in 0.25% (w/v) methylcellulose hanging drops. Kept in culture for 7 days they shrunk but keep a stable aggregated morphology.

3.1.4- Matrix embedding (Extracellular Matrix Proteins)

Since the previous results were not reasonable in terms of cells morphology, growth, survival and mainly due to the low applicability in high-throughput screenings, other culture ways were tested. Embedding cells in a matrix has been shown to bring advantages for cell growth [27], [28]. It not only gives a physical protein support that mimics the extracellular matrix present *in vivo* tumors, but is also believed to provide some protein growth stimulus.

Assays showed that embedding cells in different proteic components of the extracellular matrix gives rise to tumorspheres with different morphologies that change over time. Moreover, the type of embedding has an impact on sphere's growth and survival.

When cells are embedded in 0.25% (w/v) methylcellulose, cells show a scattered profile 24h after seeding. After one week, cells normally shrink into very compacted spheres, mainly lines D and B. At this stage line D contains several cells surrounding the main sphere, which might be an indicator of stress or death [53] (Figure 12).

Matrigel is undoubtedly the matrix that produces the most rounded shaped and smooth spheres [4], [54]. In overall, whereas 5% (v/v) matrigel results in quite compacted spheres, 1% (v/v) matrigel generates looser aggregates of cells 24h after seeding. After one week, spheres appear to have shrunk just for B line, while the others tend to keep the same diameter or eventually grow as happens with line D in 5% matrigel. Cells plated in matrigel 2.5% (v/v) acquire a similar morphology to the ones in 5%, losing the dispersed effect within 1% at 24h (Figure 12).

Moreover, a closer analysis of the spheres through time lead to the conclusion that it is necessary at least 48h for the spheres to become stable in terms of size and compression (Figure 12).

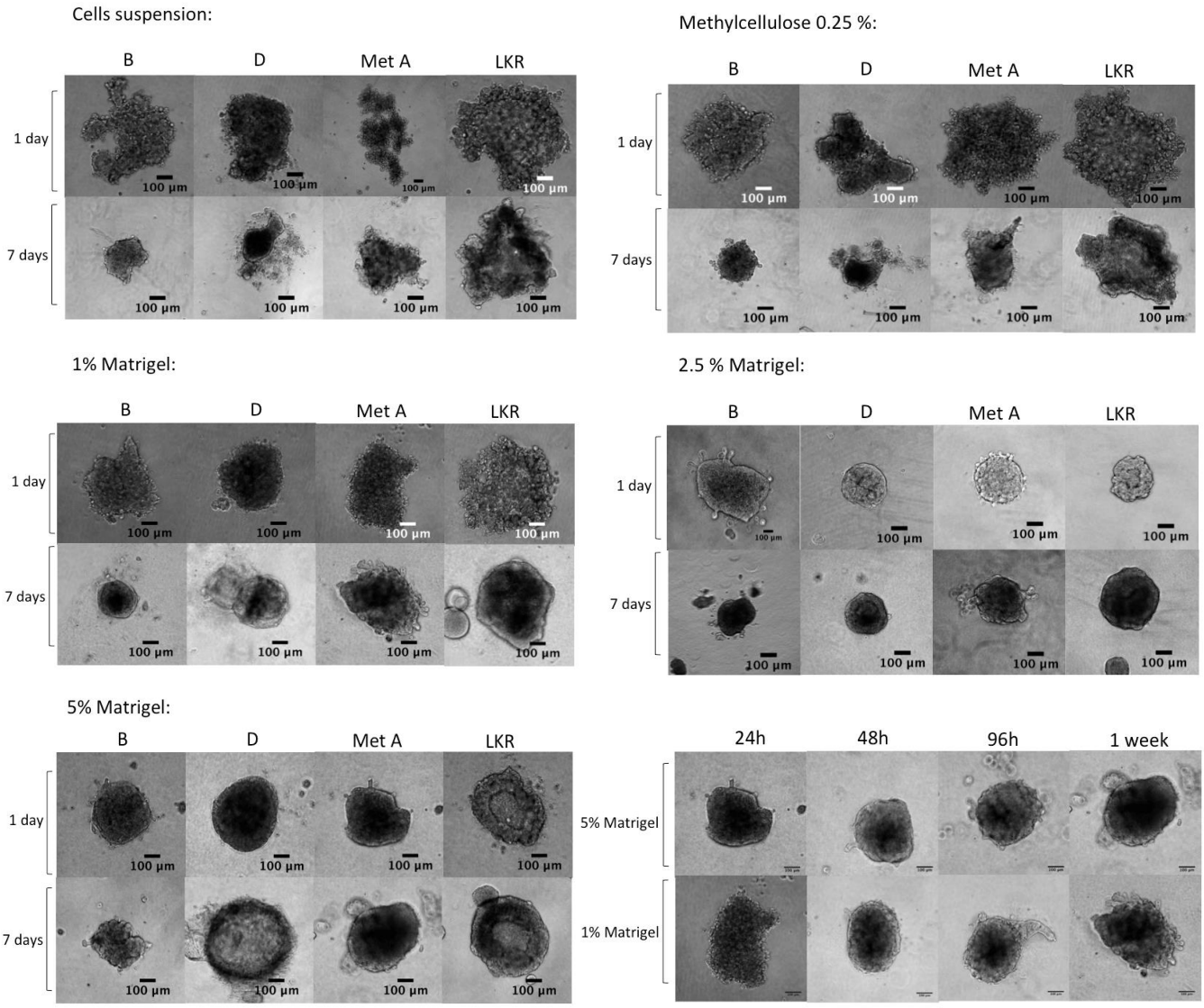

Figure 12. Matrix embedding cells have a key role in shaping morphologically better and more compact spheres. Microscopic images of several cell lines were taken when cultured under different embedding conditions. The upper left set of images is taken as a control for growth in normal media. Clear morphologic differences can be observed especially when comparing the control with matrigel embedding spheres, that apart from the negative control B line, seem to have kept the same diameter and emerge well shapely defined without dispersed cells. The lower right panel describes the time evolution of MetA line in two different conditions, revealing the size stabilization upon 48h of culturing.

Large-scale drug screenings with 3D models requires the automation of the system, which implies taking into account some robotic limitations. Among

them there is the refrigeration during the seeding, the use of only slightly viscous substances and the impossibility of removing reagents. In spite of the better appearance of cells within matrigel 5% (v/v), its viscosity is incompatible with the robotic system.

In this sense, the overall outcome of these assays have demonstrated that throughout the different available three dimensional culture methods, the one that brings better results regarding morphology, growth and ability to be used in large-scale drug screenings, are the cells growing in embedded matrix of 2.5% (v/v) matrigel.

3.2- Viability methods

Monitoring the viability of cells is one of the most important steps when doing drug assays. All the effectiveness of drugs is monitored by survival outcomes. This emphasizes the crucial importance of having a viability technique that can be as accurate and precise as possible and, at the same time, can allow the use of automatic systems for screen purposes.

Several methods were tested and compared between each other for different three dimensional culture systems.

3.2.1- CellTiter-Blue assays

One of the most commonly used viability assay in 2D cultures is the celltiter-blue assay. Its fluorescent signal results from the reduction of resazurin into resorufin by the cell redox coenzyme NADH. The signal should therefore be proportional to the number of metabolically active cells.

However, the use of the same method on 3D cultures showed that this is not a valid test. Its sensitivity is very low which might be explained by a low or null penetration of the redox dye (resazurin) into the core of spheres, disabling its reduction into resorufin by metabolically active cells. When corrected against the blank, quantification of the fluorescent signal gives a negative signal that does not correspond to the real cells viability (Figure 13).

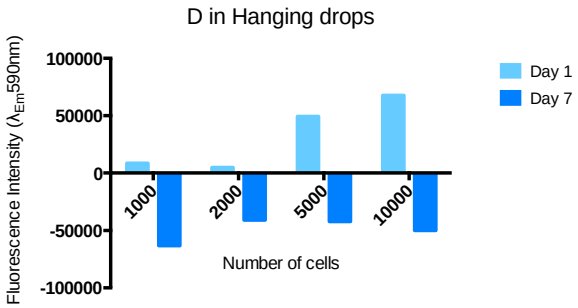

Figure 13. CellTiter blue viability assay is not sensitive to spheres. Reading resorufin fluorescence intensity on spheres cultured during 7 days gives a negative viability signal when corrected against the blank. This emphasizes the low sensitivity of the assay.

3.2.2- CellTiter-Blue with EDTA treatment

Treatment of spheres with the quelant agent EDTA has been shown to cause the disaggregation of spheres into separated cells [53]. For this reason we tested this method that overcomes the lack of sensitivity of the CTB assay alone, showing a higher fluorescence intensity signals (Figure 14).

However, microscopic observation revealed that dissociation of spheres was still not completely efficient denoting possibly that this method was still not as precise as needed, being most likely a bit misleading with elevated fluctuations. In this sense, further viability methods were tested.

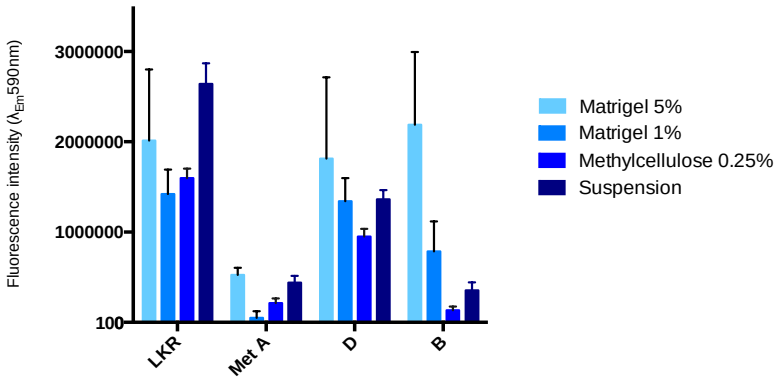

Figure 14. CellTiter blue viability assay upon EDTA spheres disaggregation disclose better results. Spheres treated for 45min with 5mM EDTA are able to dissociate and give a higher fluorescence reading.

3.2.3- Trypan blue staining

A routine method to quantify live cells is using the trypan blue staining with the cell counter, which was also used with spheroids (Figure 15). However, it is a quite tedious and manually laborious procedure that implies long incubations with dissociating agents leading to low accurate and misleading results.

Comparison of the relative values between this method and the one shown above with CTB plus EDTA for the same experiment showed no correlation (Figure 14, 15). Contrarily to CTB, trypan blue staining gives a positive growth only for LKR in 5% (v/v) matrigel, 1% (v/v) matrigel and for the control in suspension with normal media, as well as for MetA and D lines when growth takes place exclusively in 5% (v/v) matrigel. This invalidates CTB plus EDTA method that gives a high signal for many more conditions and cell lines.

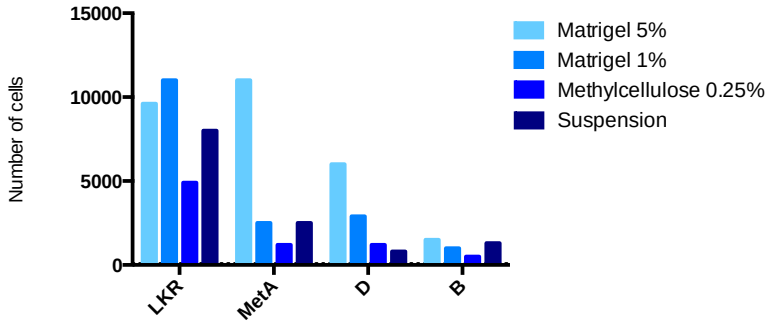

Figure 15. Viability tests with trypan blue staining do not correlate with CTB + EDTA results. The number of live cells is represented for different culturing methods and was measured with trypan blue that stains for dead cells. The overall outcome is not comparable with other viability tests invalidating those assays.

3.2.4- Integrated density of the GFP fluorescence

As described before, almost all the used cell lines are GFP positive, meaning that spheres size can be monitored along the GFP intensity signal, which should correlate with the viability of cells. Hereby, the product of the area and the mean gray pixel value of the GFP signal over DAPI stained images should give a proportion of alive cells in the sphere. Results emerge with line D having the highest integrated density for 5% (v/v) matrigel, followed by line

MetA, which bring some inconsistency regarding the previously described assays.

Most likely, this disparity may have arisen from the size and density variation of the cells over time, ending up with a higher intensity value over a smaller area, for example, fact that does not necessarily correlates with the amount of dead cells. This can be confirmed by the positive control for cells treated with staurosporin, a very toxic agent, which showed a dose dependent increase of DAPI signal, but an almost constant GFP signal (Figure 16). This indicates that the GFP fluorophore in spite of being produced only in living cells, is still active in dead cells, being able to re-emit light upon light excitation.

Moreover, this is not a simple method and cannot be used in large scale screenings. It requires a manual long analyses of each individual image as described in materials and methods. Thereby, due to the misleading results of this method, which shows a stable GFP signal upon cell death, a low connotation must be attributed to this kind of assay.

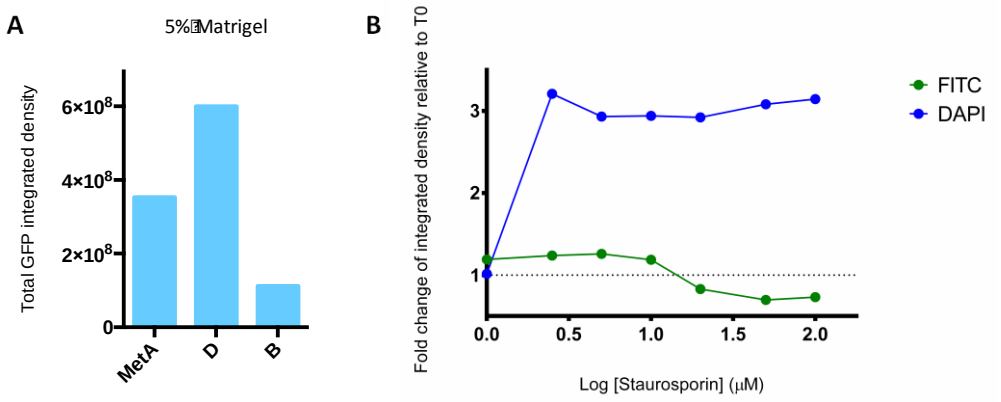

Figure 16. Total GFP integrated density measurement is an unhandy and misleading viability method. A. Total GFP integrated density of spheres cultured in 5% (v/v) matrigel. **B.** Cell death induced with staurosporin on MetA 5% (v/v) matrigel spheres. Whereas DAPI signal increases, GFP remains stable.

3.2.5- Acumen - GFP fluorescence signal

Large-scale screenings with monolayer cultures are usually monitored by the confluence of cells that gives a growth ratio regarding the control. Attempts to use this same method were made taking into account another functionality of

the same used machine: the automatic measure of the spheres area based on its intrinsic fluorescent GFP signal (Figure 17).

However, as happens with the integrated density measurements, the same problem arises due to sphere area variability, producing a high susceptibility for misleading results and low reliability.

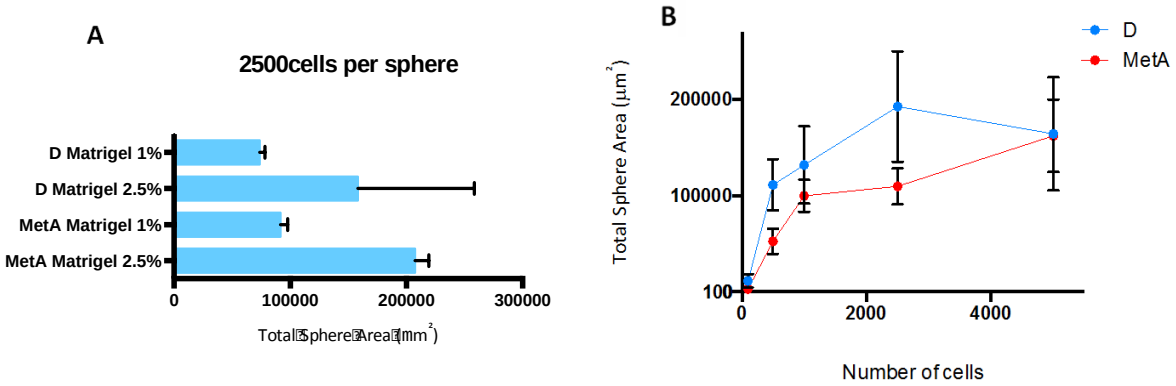

Figure 17. Total sphere area measured by acumen based on GFP signal is variable and misleading. A. Total sphere area for 2500 loading cells in matrigel 2.5 and 1% (v/v). **B.** Sphere area for different cells loading on matrigel 2.5% (v/v). There is an increase in area but the variability is high.

3.2.6- CellTiter-Glo assay

Viability tests relying in morphologic characteristics of the cells, as is its size, displayed some disadvantages. In this sense metabolic assays should be more reliable. However, the tested methods, such as CTB, have also shown low accuracy.

Some assays are now available in the market specially designed for 3D cultures. One of the available methods, the CellTiter-Glo is a luciferase based assay that measures the quantity of ATP available inside the cell, that should be proportional to the number of live cells. Its lysing properties enable it to penetrate efficiently the core of the spheres increasing the sensitive of the assay, turning the readout more realistic and informative.

Apart from the better sensitivity of this assay, and the removal of the most of the bias from the other tested assays, this is a very simple end-point method that can perfectly be used in large-scale screenings in an automatic way. Furthermore, the intensity of the signal is good, the variability is acceptable and

it shows a good proportional correlation with the number of plated cells (Figure 18).

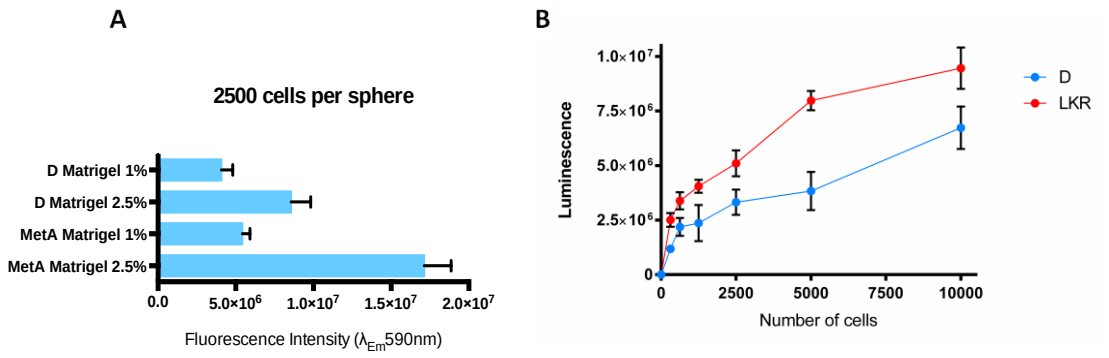

Figure 18. CellTiter-Glo viability assays shows high spheres sensitivity and low variability. **A.** Total fluorescence intensity for 2500 loading cells in matrigel 2.5 and 1% (v/v). **B.** Spheres' luminescence signal for different cells loading on matrigel 2.5% (v/v). Luminescence is directly proportional to the number of plated cells.

Regarding all the tested viability assays and for the reasons mentioned above, CellTiter-Glo is undoubtedly the most reliable one, and so it was chosen for the following assays.

3.3- Outlook – viability of 3D culture

A drug screen with spheroids brings certain limitations that need to be overcome. Experimental design needs to be ensured for each different cell line to guaranty the reproducibility of the assay. Hereby, a standardized protocol with a consistent spheroid size needs to be taken into account as well as the microsatellites often observed in 3D cultures need to be discarded. This will reduce the variability of the tests and bring more accurate results with better analysis. Spheres size variability implies different core oxygenation and nutrient uptake, resulting in different gradients generally similar to *in vivo* tumors [55]. These oscillations also establish protein expression levels and proliferation rates, which are expected to result in different therapy responses comparing to 2D drug screenings [28].

In this sense, setting up the best conditions to culture cells in a three dimensional way compatible with drug large-scale experiments, needs to be easy to handle, be very consistent, ensure cell growth and survival through at least one week and finally its viability needs to be accurately monitored.

For this reason, it was then important to test again the different 3D culture methods with the CTG assay and evaluate cell growth over time (Figure 19).

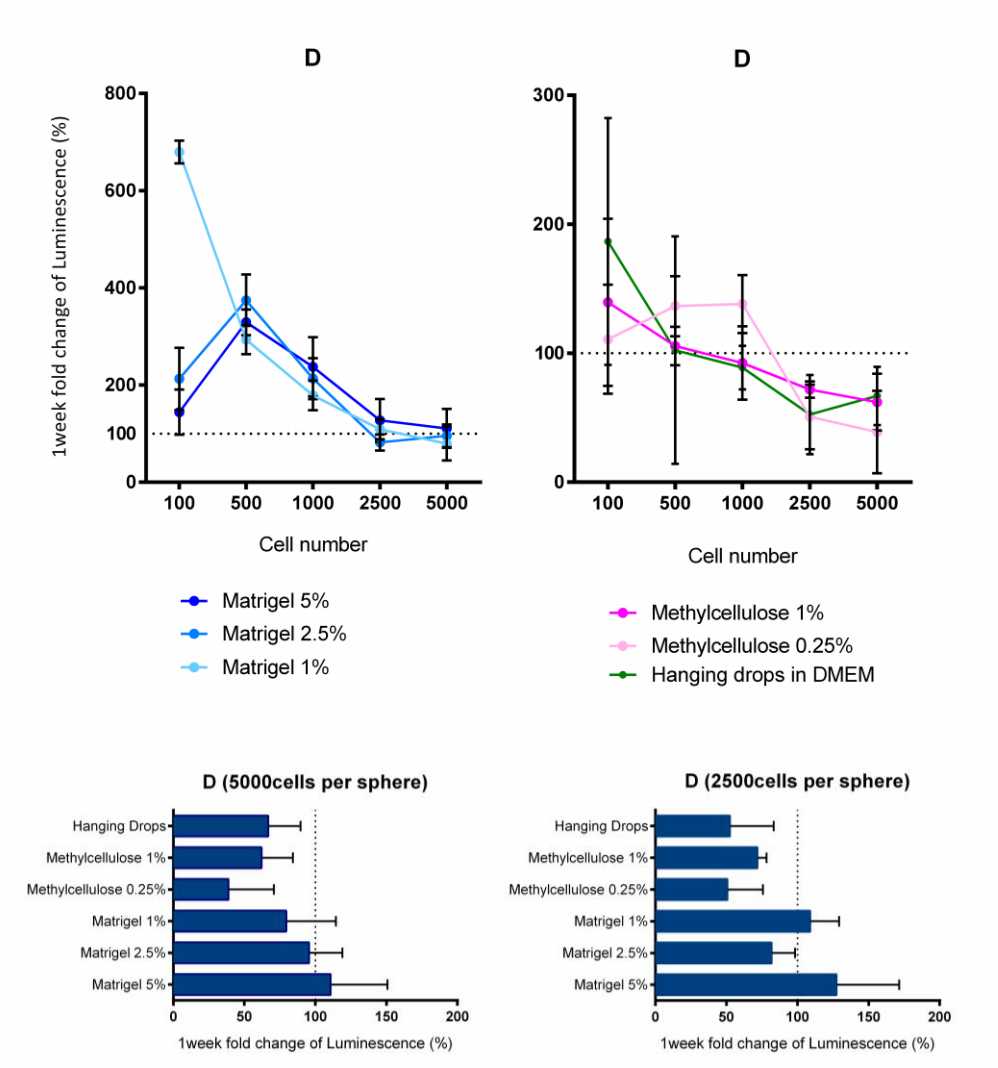

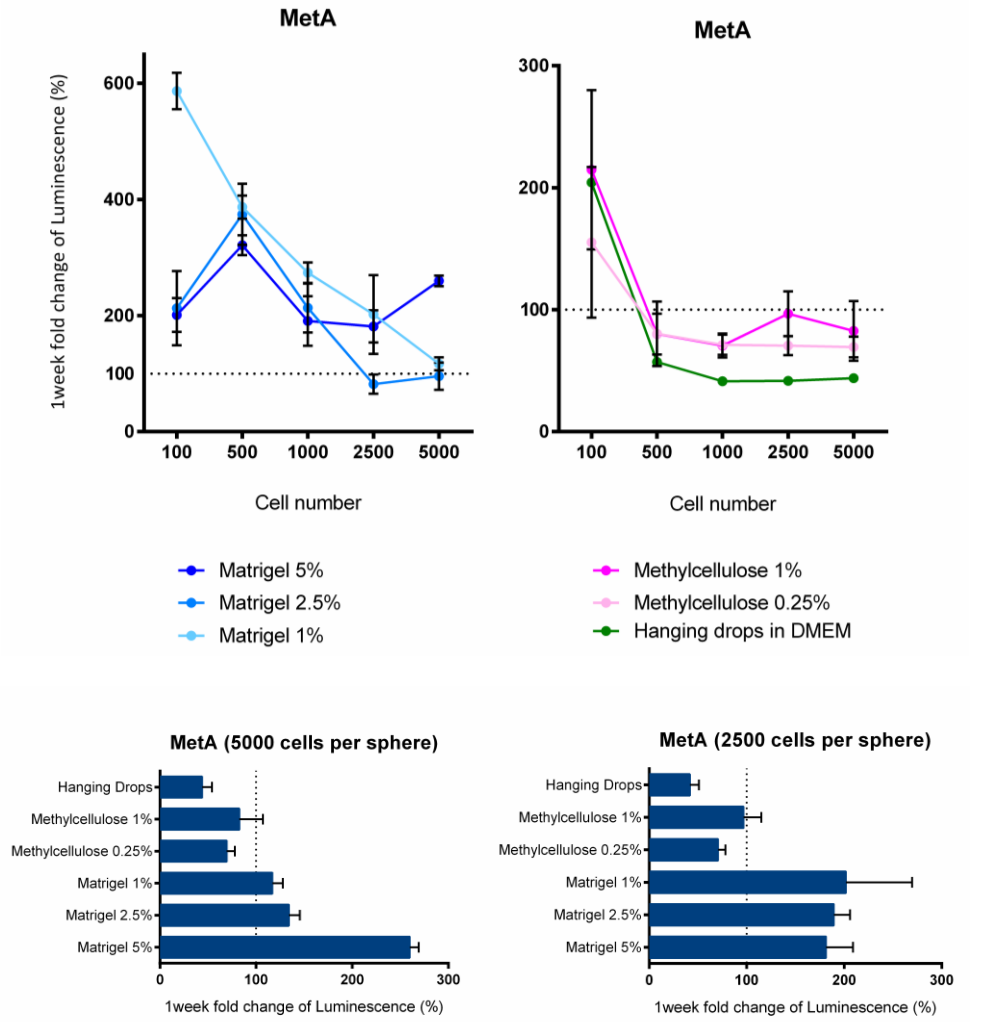

Figure 19. Embedding spheres in matrigel express the higher cells' survival and growth rates over one week. Linear graphs show 1 week fold change luminescence for lines D and MetA cultured under different methods for variable cells loading. Bar graphs show the viability fold change for the different methods over one week for a fix cell number. Matrigel shows the best results with positive growth after one week.

As already seen in the previous assays, the outlook from the viability in the course of 1week throughout the different 3D culture plating techniques, points out how matrigel has a clear importance on the growth and culture maintenance of the NSCLC MetA and D lines.

These results discard the use of methylcellulose as a successful matrix for long-term cell growth as well as the hanging drop. Having in consideration the robotic limitations for large-scale screenings and the outcome from the analysis of the different techniques, 2.5% (v/v) matrigel appears as the best option.

Apart from the 3D methodology, consistency cannot be reached without the determination of the best cell loading. CTG oxyluciferin fluorescence signal

shows to be dependent on the amount of seeded cells. Line D is a good model on how the curve slope tends to be bigger for the lowest amount of cells, stabilizing above 2500 cells. Cells maintained in 5% (v/v) matrigel show a viability decrease between 48h and 96h after plating, recovering considerably after one week on both tested cell lines, MetA and D. This decrease can be associated with a natural selection for the most non-anchorage dependent cells, allowing them to start growing much more afterwards (Figure 20).

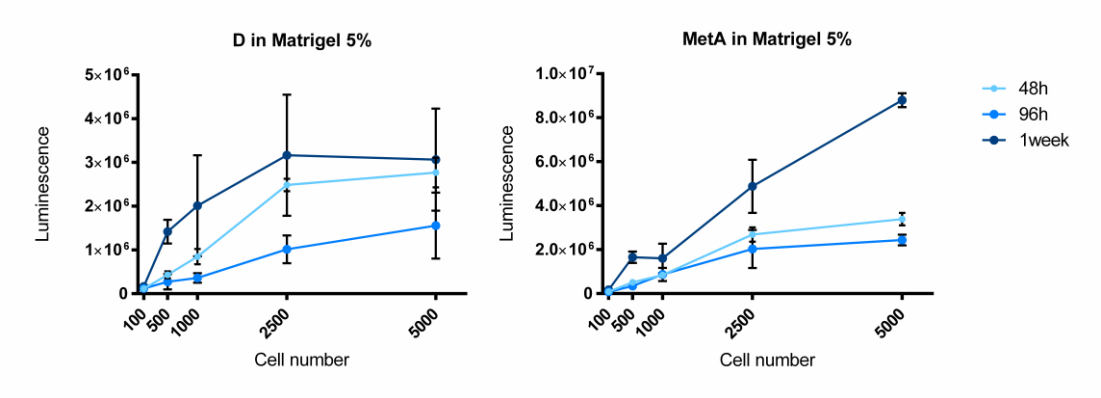

Figure 20. Luminescence is mostly proportional to a cell loading bellow 2500 cells. Variation of luminescence through time according to the number of plated cells in matrigel 5% (v/v). A stabilization of the luminescence signal is observed above 2500 cells mainly for D line.

In this way, 2500 cells seem to show the best results. The saturation of the system is avoided and drug tests are more likely to work, generating more trustworthy results. Cells will have around 300µm of diameter, forming a gradient of nutrients and oxygen, that is observed *in vivo* tumors, allowing at the same time drugs to penetrate the core, eliminating possible false negatives in drug screenings.

Altogether the described results have defined the best conditions to be used for all the following experiments. 2500 cells need to be seeded in 2.5% (v/v) matrigel and drug assays should be started after 48h. Ultimately, viability of cells should be monitored with CTG assays.

3.4- Morphology of the spheres

The all purpose of growing cells in a three dimensional way, lays on the total surface interaction between cells alike the *in vivo* situation. The morphology of cells was analyzed by several resources to understand the general organization of the spheres and to get further insights about the existence of connections between cells.

3.4.1- Transmission electron microscopy (TEM)

The spatial organization of the spheres was monitored by TEM either after 48h or one week upon seeding. Cells in 3D cultures display a very healthy morphology, with normal organelles, especially plenty of mitochondria, golgi apparatus and lysosomes (Figure 21A).

Indeed, in one week, structural modifications and connecting interactions are evident especially in D line spheres. It shows a curious particular phenotype: Cells differentiate into other cells with different organelles and structures, that may be important for nutrient uptake; they specifically form structures similar to acini characterized by the presence of microvilli cells with tight junctions only at the top of the cells facing the lumen of the acinus; gaps are certainly fulfilled with matrix secreted by these microvilli cells, probably playing a role on their survival; Numerous linkage structures like adhesion junctions and desmosomes are also present (Figure 21).

This interesting organizational fact is just present in 3D culture, whereas in 2D they have just cells with very short and rare microvilli (Supplementary Information 1). This denotes the exclusive potential of 3D culture cells to differentiate and change its structural organization.

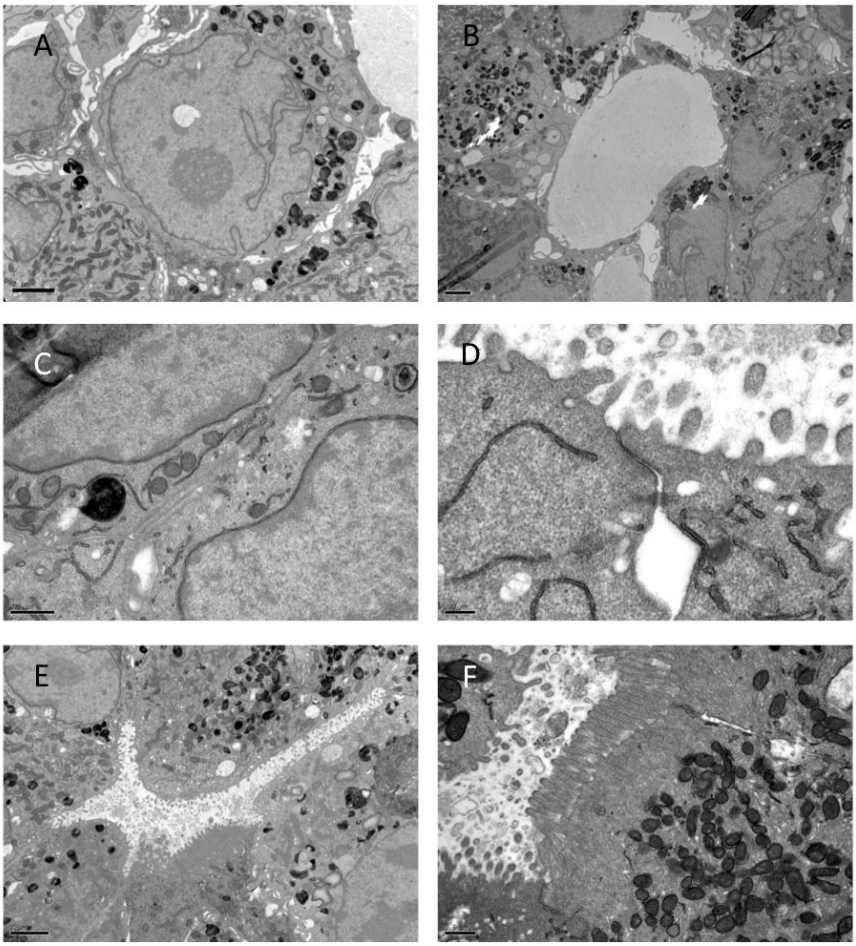

Figure 21. TEM images for D line. A. D line shows an healthy morphology and organelles anatomy. With lysosomes, mitochondria and golgi very often observed. **B.** Gap filled with matrix secreted from cells. **C.** Adhesion junction **D.** Desmosome on top of the cells facing the acini lumen. **E.** Acini. **F.** Long microvilli facing the acini lumen.

The scenario changes for the other cell lines. On B line, cells are tightly packed but arranged randomly. It is very difficult to see junctions between cells, just cell-to-cell contacts. There are no tight junctions, no villi and the presence of desmosomes is dubious (Figure 22). On the other hand, LKR line shows lots of gaps between cells and no arrangement into structures. There exist lots of short villi that are probably just random protrusions from cells. There are cell-to-cell adhesions at random places but little tight junctions are observed. The occurrence of desmosomes is also not clear (Figure 23). MetA line that was screened 48h after seeding has many gaps between cells but no villi. There are adhesions at random places but it is hard to find junctions as well as desmosomes (Figure 24).

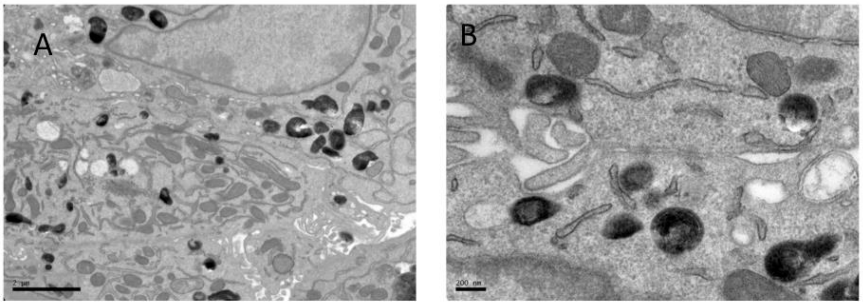

Figure 22. TEM images for B line. A. Tightly packed and randomly arranged cells. **B.** A possible desmosome.

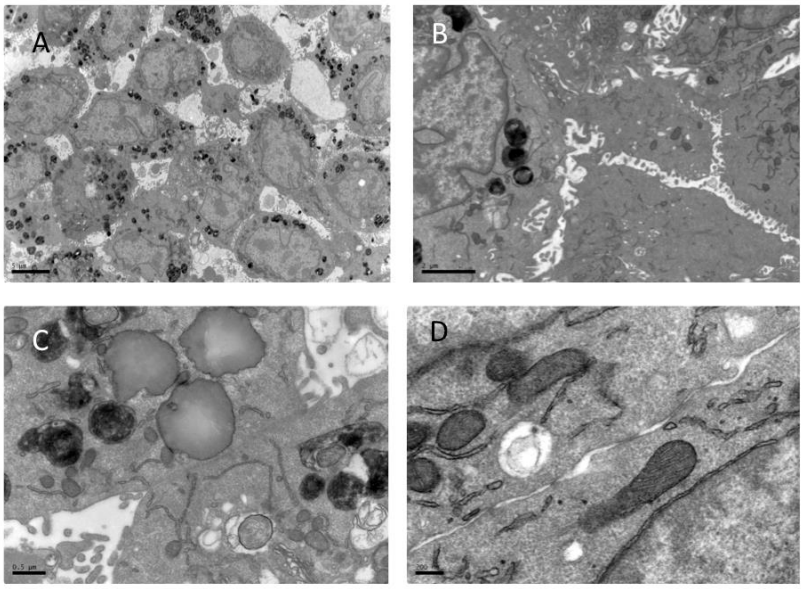

Figure 23. TEM images for LKR line. A. Many gaps between cells. **B.** Short microvilli. **C.** Adhesion junction seems to appear in random places. **D.** A possible desmosome.

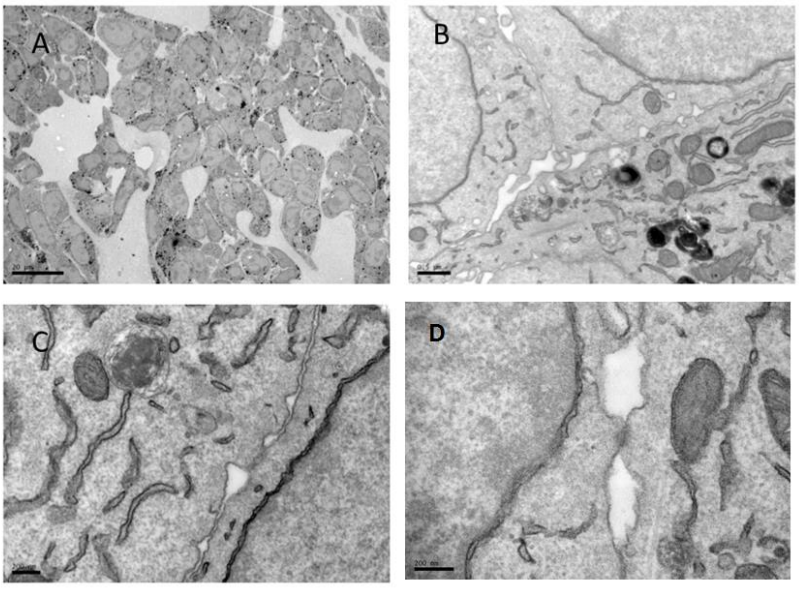

Figure 24. TEM images for MetA line. A. Gaps between cells. **B.** Adhesion junction. **C.** Randomly placed adhesion junction. **D.** Desmosome

3.4.2- Electron microscopy (EM)

For an external point of view spheres were also examined by Electron Microscopy (EM). They all look very well packed together and surrounded by fibers of matrigel. The outer layer has a very smooth appearance and cells are completely linked to each other. Lines D and LKR are completely covered with micro-protrusions whereas MetA line is totally covered by matrigel, which makes the surface analysis more difficult (Figure 25).

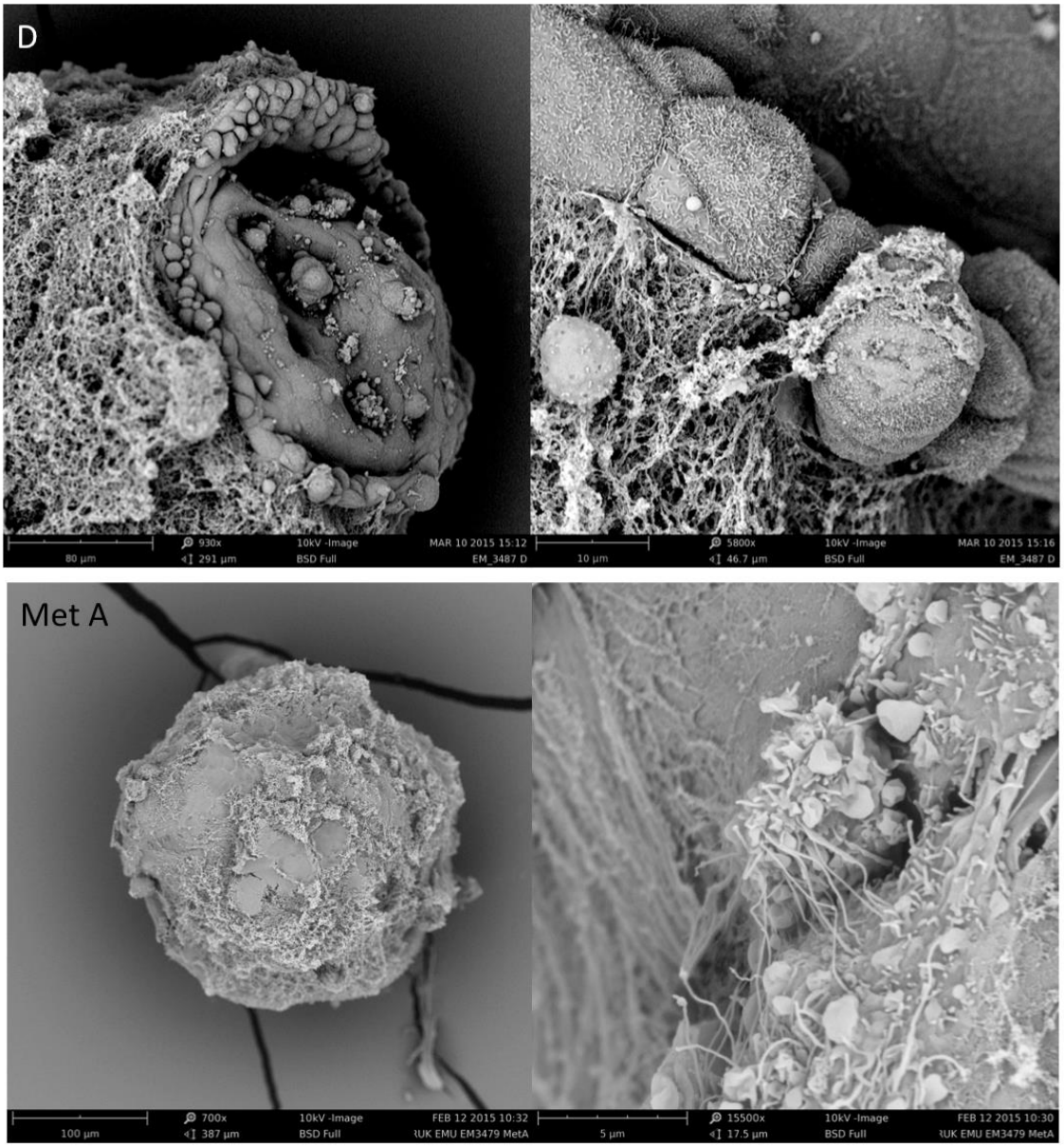

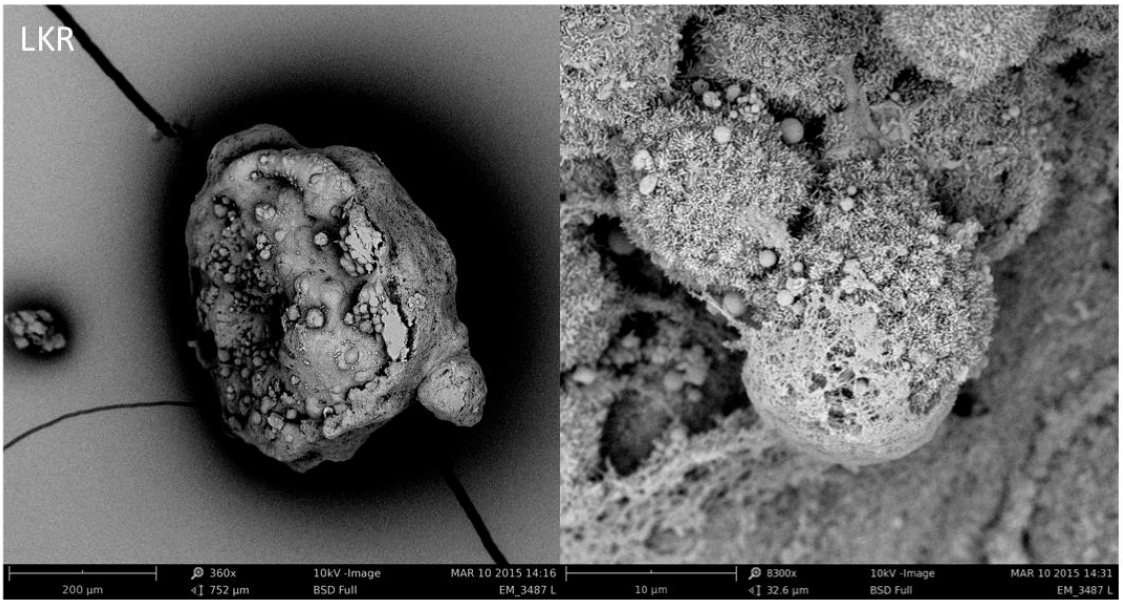

Figure 25. EM images of D, MetA and LKR spheres. Spheres appear very well packed and surrounded by matrigel fibers.

3.4.3- H&E and E-cadherin marker

TEM and EM microscopy gave an overview of the structural organization of the cells, but to better understand how exactly cells are ordered within the sphere, E-cadherin expression pattern was also analysed by immunohistochemistry. Haematoxylin and eosin (H&E) staining was used as a control.

E-Cadherin staining is positive for D and LKR lines, revealing cell differentiation and organization. D line forms acini E-Cadherin positive inside the sphere, as was already observed by TEM, whereas LKR as a strong positive signal just in the apical surface. H&E staining also shows in pink that in D line gaps are filled with some extracellular matrix secreted by cells. This means that, contrarily to LKR, line D lay down on its extracellular matrix. E-Cadherin is negative for MetA line, possibly justified by its metastatic derivation, with higher invasive potential (Figure 26).

Similar results were already published by *Vertrees et al* on BZR-T33 lung cell line (H-*ras* transfected BEAS-2B). Here, 3D cultures showed a higher degree of differentiation and marker expression more closely related to cells grown in situ, when compared to monolayer cells [25].

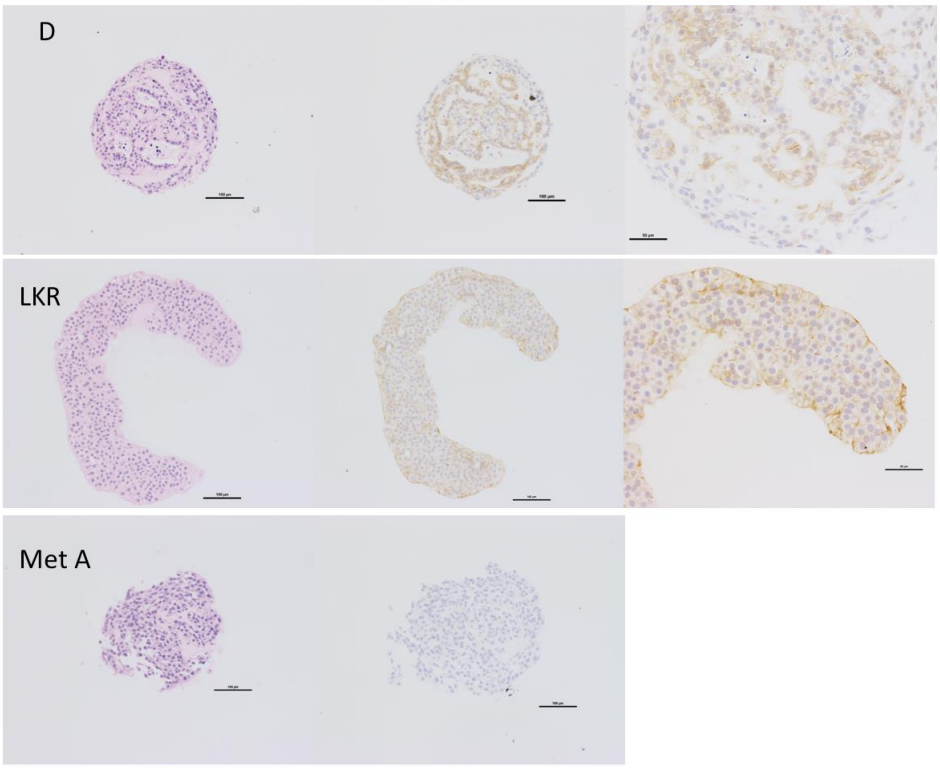

Figure 26. H&E and E-cadherin staining. H&E can be seen on the left side for the different spheres and on the middle and right side immunohistochemistry staining for the cell adhesion protein E-cadherin is demonstrated.

Morphologic analysis of the spheres cultured in 2.5% (v/v) matrigel, showed a curious phenotype for D line, with evident differentiation upon only one week culturing, forming acini E-cadherin positive. Lines MetA and LKR are not as well organized as D line, but these ones still connect with each other through junctional complexes such as adhesion junctions and desmosomes. As expected, MetA cell line does not present the E-cadherin marker most likely because it is a metastatic line, and it is known that loss of this marker can increase the invasiveness potential of these cells [56].

Altogether, the morphologic analyzes of the spheres had shown that, in general, spheres tend to form connections between each other. All the analyzed cell lines appear to have adhesion junctions. It indicates that spheres might indeed work and function as a multicellular organoid, swapping signals, stimulus and some factors. D line showed particular features, it is able to activate some differentiating functions, showing a very organized structure, with acini, microvilli. It is also E-cadherin positive for the cells facing the lumen of the acini and for the cells facing the apical side of the spheres.

3.5- Signalling Pathway

Cells display morphologic differences depending on the way they are cultured. Addressing now whether these differences imply any impact on the activity of KRAS signalling pathway becomes a focus of importance.

Indeed, when checking for the levels of Akt, Erk and MLC activation, all enrolled at the RAS protein cascade, there is a major difference in the levels of p-Erk that are twice higher in 3D cultures when comparing to 2D (Figure 27). Erk activation is known to be related with the higher potential of proliferation [57]. The Western-blot results indicate that cells growing in 3D either from a metastatic cell line as MetA as well as the KRAS mutant $p53^{-/-}$ D cell line, are more predisposed to proliferate. On the other hand, there is no difference between 2D and 3D cultures for p-MLC levels, which are known to be involved in cells motion [58]. Cells in 3D cultures tend to be confined to a single and unique sphere, they may be able to grow in volume and density, but usually the previous results gives the impression that they hardly grow in size, mainly when the number of loaded cells is superior to 2500. These results indicate that cells are as prone to move in 3D as they are in 2D cultures (Figure 27).

Regarding the levels of p-Akt, there is no correlation between the two culture methods and the differences are not significant, being the Akt activation very low. p-Akt is an indicator of cell surviving and nutrient sensing [59]. Results indicate that most likely cells do not rely on p-Akt signalling pathway (Figure 27).

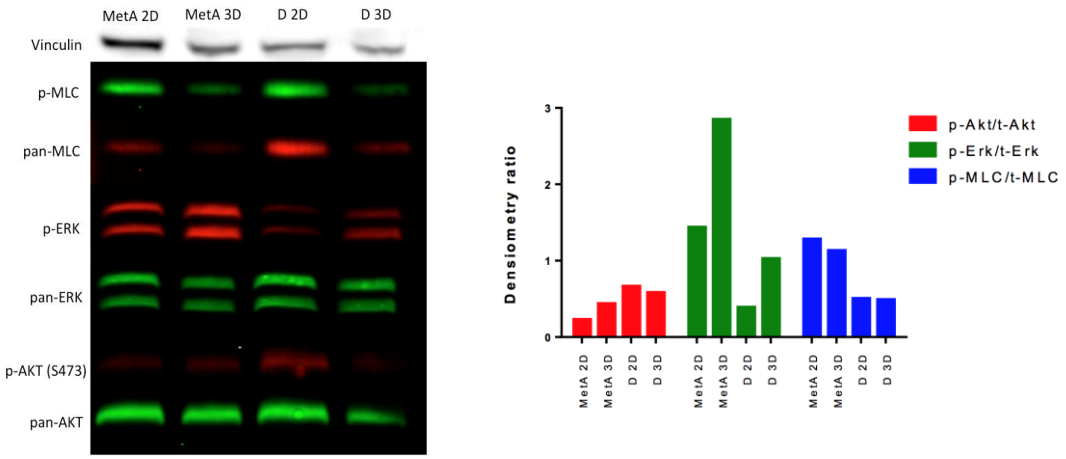

Figure 27. Differences in the signalling pathway between 2D and 3D cultures. Whereas Akt and MLC activation levels remain quite consistent for both culture methods, p-Erk levels tend to be increased in 3D cultures for MetA and D lines.

Results suggest that 3D cultures tend to have the MAPK pathway more active because of the higher levels of p-Erk.

3.6- KRAS sensitivity – 2D *vs* 3D

After the determination of the best conditions required to grow spheroids from NSCLC an interest to further investigate different sensitivities towards targeted therapies arose. We have shown that cells grown in 3D show morphological differences as well as variations in the expression levels of certain proteins compared with 2D cultures. There are also reports in the literature showing that 3D cultures tend to simulate more accurately the gene expression profiles in clinic, as well as the pathophysiological milieu in cancer patients demonstrating closer therapy responses. This may in turn improve clinical efficacy prediction of therapies, revolutionizing antitumor screening operations [27], [28].

In this sense, it becomes essential to test the efficacy of chemical compounds known to interact in the oncogenic KRAS signalling in order to predict its outcome in a more realistic culture method that are 3D platforms, analyzing whether major differences can be found between the two culture systems.

3.6.1- Preliminary drug screen

Published data already reported that 3D cultures are expected to work in two ways: some drug candidates may lose efficacy in 3D assays, discarding further animal tests and eventually pull up its optimization; and others may exclusively be effective in 3D cultures.

In this way, 3D drug screenings can indicate which chemical compounds should be followed up for later trials because of its potential to better estimate *in vivo* antitumor efficacy [28].

A preliminary 3D drug screen was then made in MetA cell line using a kinase inhibitor library. Results obtained were analyzed and compared with a previous screen done in the host lab in 2D cultures with another cell line. 348 compounds were used in a 10µM concentration as single replicates. Total sphere area was monitored by its intrinsic GFP fluorescence signal through a 6 day period following treatment.

A massive sphere area variability is observed in the control samples, mainly at day 6, whereas pretreated cells have minimal variations. Moreover, a 72h drug treatment shows a smaller variation in regard to a 6 day treatment. This is certainly explained by the different growth rates brought up through time by minimal loading errors, the presence of misleading microsatellites or even by differences in the growth conditions within the same 384 well plate. These results highlight the complexity in the standardization of the 3D procedure even after consistent results in small scale assays (Figure 28). Data was selectively analyzed taking into account the viability range of positive and negative control drugs, and upon categorization into drugs with cytostatic, cytotoxic and growth effects, 10 hits were identified. Such hits were exclusively drugs which performed opposite effects regarding 3D and 2D cultures, failing to show efficacy in 2D and being highly efficient in 3D (Table 1).

It is worth pointing that 2D data were extracted from a total independent experiment with a different cell line. *A priori*, it is known that this comparison can mask some potential effective drugs and can lead to contradictory results once done with the same cell line. The screen was done in the high-throughput screening facility with the objective of determining if the method could be automated and used in a high throughput fashion. Although we can take some information from it, ideally we should repeat it using at least triplicates for each point and comparing at the same time the 2D and 3D cultures.

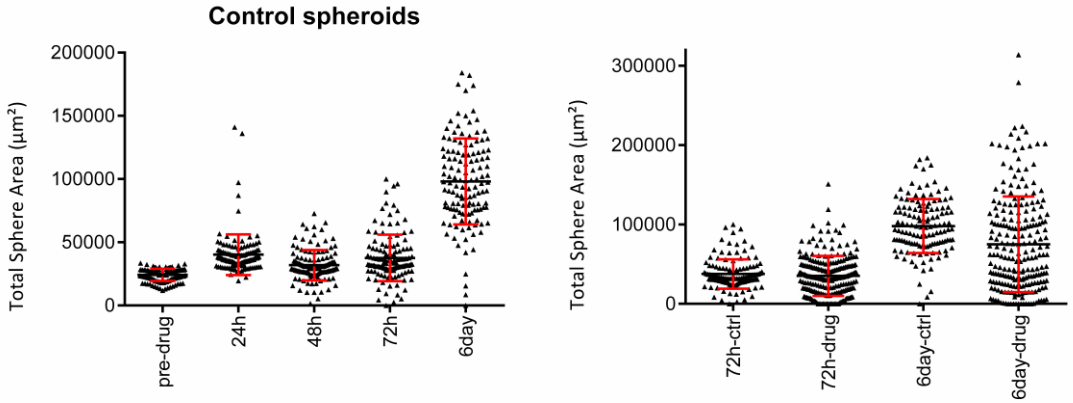

Figure 28. Preliminary screening variability on MetA. The left chart represents the spheres' size variability just for the untreated spheres over time. A variability range of about 10.000μm^2 is reach on day 6. The right chart shows the comparison of size variation between treated and non-treated spheres. Each dot represents one single sphere treated with one of the 348 used compounds with respective control sphere upon 72h and 6 days of treatment.

Table 1. Top 10 hits identified after screening. From the kinase inhibitors library, 10 compounds shown to be effective on 3D MetA cultures. Whereas, on an independent experiment with a different lung cancer cell line cultured in 2D, the same ones had a growth effect.

Compound	Description	Day 6 - Viability fold change % (3D – MetA)	Viability fold change % (2D)
Gš 6983	PKC inhibitor	-100	109.8
IKK-2 Inhibitor VIII	IKK-2 inhibitor	-100	88.9
TGF-β RI Inhibitor III	Inhibitor of ACTR-IB, TGF-β RI and ACTR-IC	-100	85.2
Indirubin-3′-monoxime	GSK-3β and CDK inhibitor	-84.8	51.2
GSK-3β Inhibitor XII, TWS119	GSK-3β inhibitor	-65.8	55.1
LY 294002, 4'-NH2	PI3K inhibitor (p110α, p110β, p110δ, and p110γ subunits)	-44.5	88.0
Isogranulatimide	ChK1 inhibitor	-44.2	96.7
IKK-2 Inhibitor IV	IKK-2 inhibitor	-38.3	44.0
Compound 56	Inhibitor of the tyrosine kinase activity of the EGF	-32.3	74.5
PI 3-Kα Inhibitor IV	PI 3-kinase family inhibitor	-31.0	54.1

Taking into account the best drug candidates from the preliminary screen, further tests were done at small scale comparing the same cell line in 2D and 3D cultures (Figure 29). Cell viability was monitored with CTG assay 72h and 6 days upon treatment. D line revealed to be quite sensitive for all drugs disregarding the culture method. The exception lays on the PD0332991 dihydrochloride (CDK inhibitor), that upon 6 days of treatment showed a significant increase in the viability levels for 2D cells but not 3D, indicating that 2D cells are less sensitive for this inhibitor. On the other hand, MetA line did not follow the expected pattern from the screening. It rather showed a better 2D effectiveness for BMS-345541 (IKK-β inhibitor) and Gö7874 (PKC inhibitor) drugs. PD0332991 dihydrochloride treatment had the expected effect, however not as strong as the screen.

Results showed that there are differences between 2D and 3D, but that these differences also differ between both cell lines. The exception is the CDK inhibitor that has the same response on MetA and D lines. Therefore, there is a need to generate uniform spheroid fractions to reduce variability [28], [60].

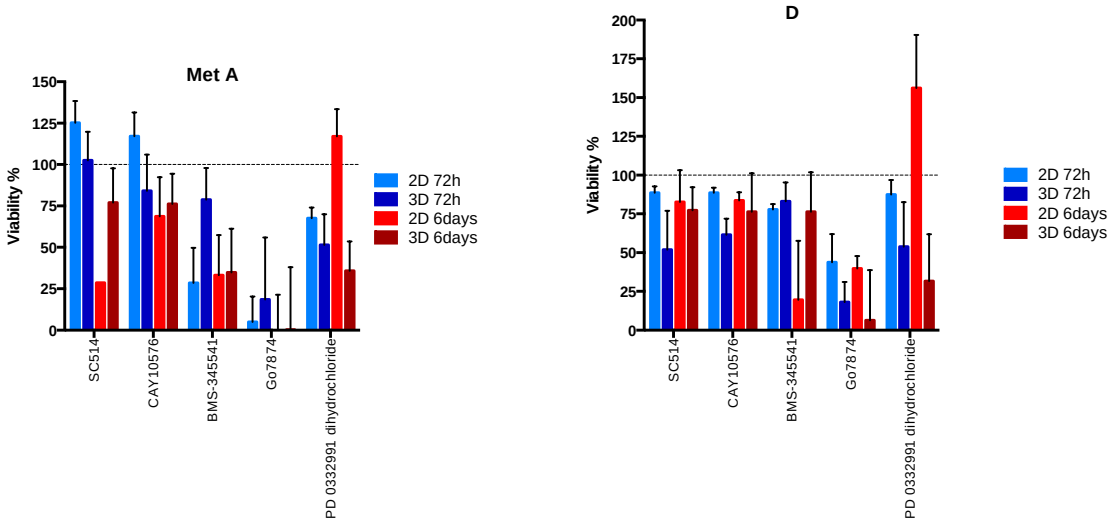

Figure 29. 2D and 3D viability upon treatment with 5 of the best drug candidates from the screen. 6 days of treatment with the CDK inhibitor PD0332991 dihydrochloride had a big impact on 3D cells viability for D and MetA lines whereas a considerable growth was observed for 2D cultures in both cell lines.

Results with the most divergent viability percentages in both cell lines were then followed up to dose response assays with respective IC_{50} determination for both culture methods (Table 2).

Dose curves follow different patterns. IKK-β inhibitor forms bigger slopes on 3D cultures, but the IC_{50} does not diverge significantly. However, at the highest drug concentrations, cells tend to reach the same levels of viability, being therefore affected by the same range of death (Figure 30).

Previous reports had demonstrated that effectiveness of IKK-β inhibitors on $KRAS^{G12D}$ induced lung cancers, is higher when they are tumor suppressor p53 deleted [17]. Assays are according to literature showing a high effectiveness on MetA and D lines but not LKR, which is KRAS mutant alone. For all cell lines, 2D showed to be a more sensitive culture model.

Looking at the IC_{50} values along with the graphics, differences can be observed between 2D and 3D cultures with the PKC inhibitor Gö7874. LKR and

D lines are much more sensitive to this inhibition when cultured in monolayers, being spheres modestly more resistant.

Table 2. IC_{50} values for IKK-β, PKC and CDK inhibitors on 2D and 3D cultures. LKR and D 2D cells are significantly more sensitive to the PKC inhibitor Gö7874 than 3D cultures. NA means that cells did not reach IC_{50}.

		MetA		LKR		D	
Name	**Description**	**2D**	**3D**	**2D**	**3D**	**2D**	**3D**
BMS-345541 (μM)	IKK-β (IKK-2/IKBKB) inhibitor	0.6	1.1	1.6	2.3	1.2	1.4
Gö7874 (μM)	PKC inhibitor	0.25	0.3	0.25	1.2	0.7	2.6
PD0332991 dihydrochloride (μM)	CDK inhibitor - high selectivity for CDK4 and CDK6	1.7	1.1	0.7	NA	NA	7.2

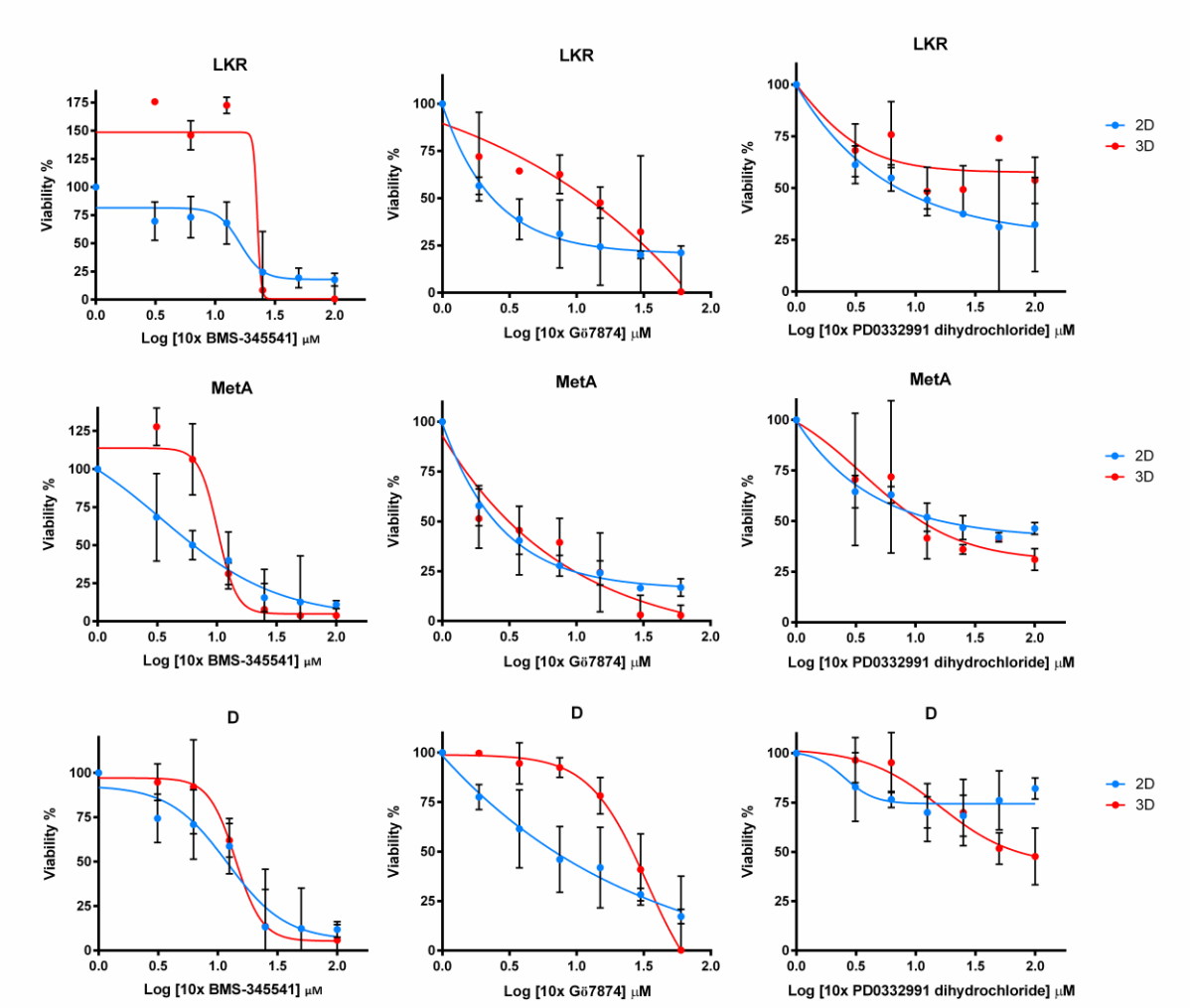

Figure 30. Dose effect of IKK-β, PKC and CDK inhibitors on 2D and 3D viability upon 72h treatment. Different responses can be observed between 2D and 3D cultures mainly for the PKC inhibitor Gö7874 and the IKK-β inhibitor BMS-345541.

Results obtained show that PKC inhibitor can produce more pronounced differences between the two culture methods, being quite more effective to 2D cultures whereas 3D cells acquire a certain resistance. This demonstrates that the efficiency of some drugs can vary depending on the growth conditions.

3.6.2- KRAS target drugs

As it was detailed before, cancer arises when normal growth regulation breaks down. RAS proteins are key regulators of cell growth controlling signalling pathways. RAS oncogene is capable of redirecting input signals to alternative pathways. This constitutively activates certain pathways, leading to higher amounts or high functional activity of transcription factors. Direct KRAS therapies have brought poor effectiveness. Additional mutations, either upstream or downstream of the pathway turned out to bring poor clinic prognosis [10], [16]. In this sense, targeting novel proteins involved in the process becomes crucial.

Thus, a set of inhibitors known to be effective in 2D cultures was used at this time also in 3D cell models in an attempt to find different vulnerabilities between 2D and 3D cultures for RAS mutant cells.

3.6.2.1- MEK and PI3K inhibitors

Cells are strongly sensitive to MEK inhibitors both in 2D and 3D without major differences between methods apart from LKR cell line, which clearly showed to be less sensitivity in spheres (Figure 31).

PI3K inhibitors were also used to block AKT/PI3K parallel pathway, known to be activated by RAS. Indeed, they were effective for all tested cell lines (Figure 31). Although, major differences were noticed between 2D and 3D methods on D line, that comes with a lower IC_{50} for 3D cultures indicating higher sensitivity of these cells. These results can be supported by morphologic reasons. Line D survival might rely on external stimulus [21] that propagate much better when cells are closely pack together with a bigger membrane surface. On the other hand, LKR and MetA appear to be more sensitive to PI3K inhibitors on 2D cultures, with an IC_{50} four times lower for MetA (Table 3).

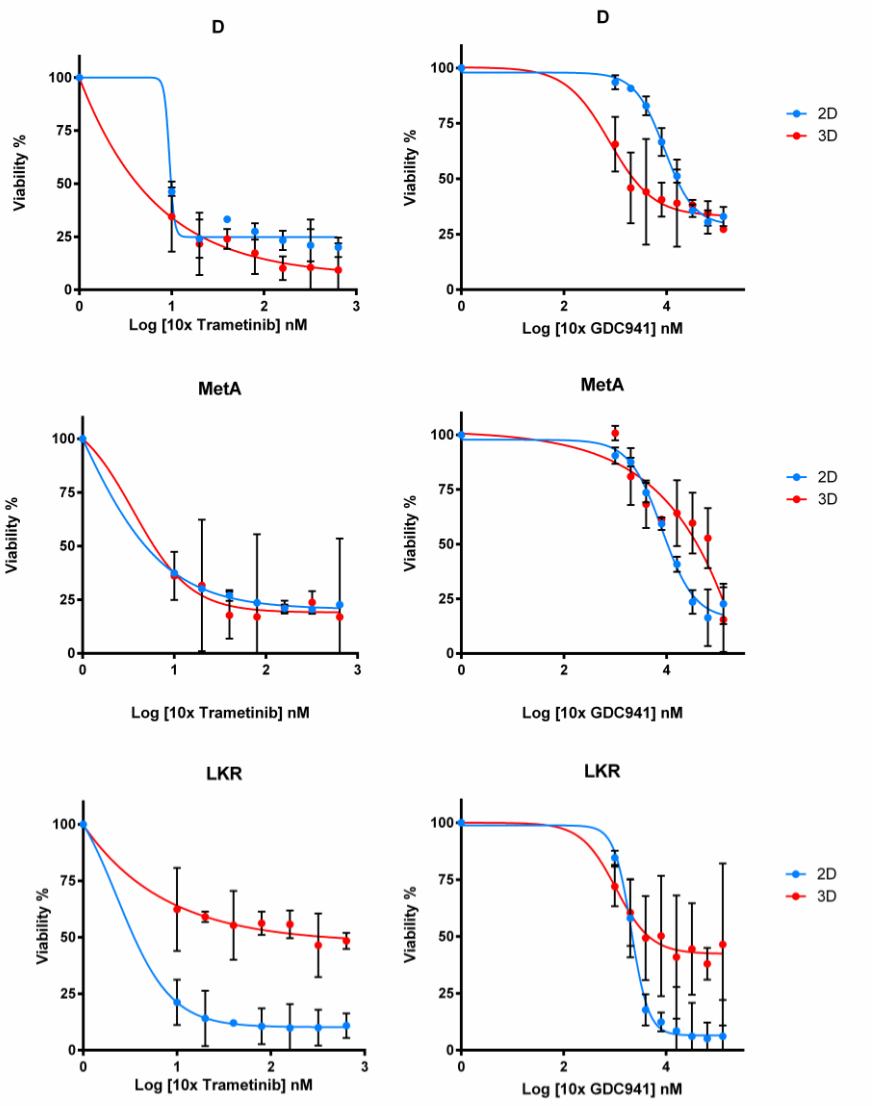

Figure 31. Dose effect of MEK and PI3K inhibitors on 2D and 3D viability upon 72h treatment. Clear different responses can be found between culturing methods for MEK inhibitor Trametinib in LKR line and PI3K inhibitor GDC941 in D line.

Table 3. IC_{50} values for MEK and PI3K inhibitors on 2D and 3D cultures. LKR 2D cells are more sensitive to Trametinib. GDC941 brings more sensitiveness for 2D MetA cells and 3D D line cells.

IC_{50}		MetA		LKR		D	
Name	**Description**	**2D**	**3D**	**2D**	**3D**	**2D**	**3D**
Trametinib (nM)	MEK inhibitor	0.5	0.6	0.3	43	1	0.4
GDC941 (nM)	PI3K inhibitor	1040	4000	220	460	1560	225

These results bring to light that the LKR line is less sensitive to the main pathway MEK and PI3K inhibitors when cultured in spheres. PI3K inhibitor is more effective on 3D cultures for the D line, but the opposite happens for MetA, indicating a cell line response dependency. Once more we see here that differences between 2D and 3D do exist, but they are dependent on the cell line.

Taking into account the different sensitivities upon MEK inhibition, the respective signalling pathways were analysed (Figure 32). The reduced levels of p-ERK upon treatment indicate that Trametinib is working on spheroids. P-ERK is not detectable on non-treated 2D cells, but increasing levels of p-MEK after 8h treatment confirms a positive feedback loop due to MEK inhibition. Conclusions about the different sensitivities between 2D and 3D cannot be made with this western blot assay, once it does not display major differences between both cell lines and the signal for p-AKT was too low. However, the lower levels of NF-kB upon 8h treatment of D line in 3D may be responsible for the higher sensitivity of these cells towards Trametinib, as it is also confirmed by its lower IC_{50}. The D line is then probably relying more on NF-kB pathway when it is cultured in 3D conditions.

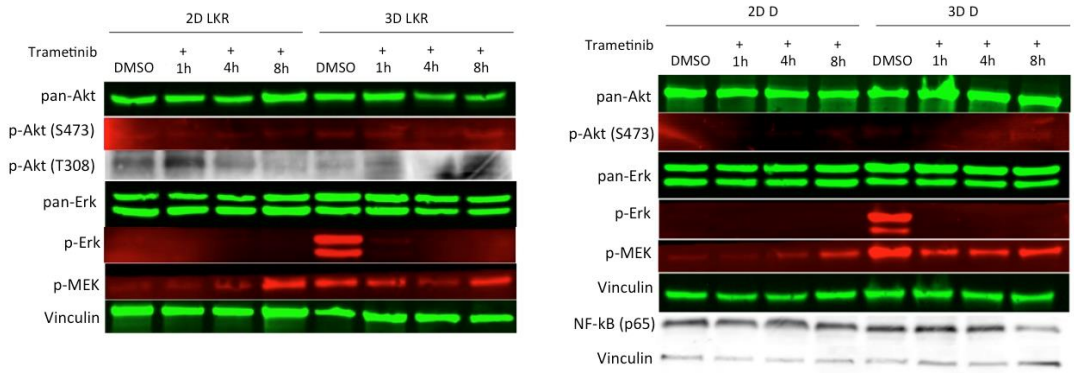

Figure 32. Effect of MEK inhibitor on signalling pathway for 2D and 3D cells over time. 72h upon treatment with the correspondent IC_{30} dose, lysates were blotted against the indicated proteins. As expected, Trametinib is having an effect on p-ERK levels but no differences between D and LKR lines are able to explain the observed different drug sensitivities. NF-kB (p65) levels are shown for D line. The decreasing levels upon 8h for 3D cultures indicate a higher dependency of this type of cultures from this signalling pathway.

Further studies are needed in order to understand how differently these inhibitors may affect the pathway accordingly to cells morphology and spatial

disposition. Therefore, western blot optimization along with a more efficient sphere protein extraction is required to achieve detectable p-AKT levels.

3.6.2.2- Other inhibitors

Proteasome inhibition by Bortezomib, a drug already used in clinic, is totally effective with minimal doses and no major differences were found regarding the culture method used (Figure 33, Table 4).

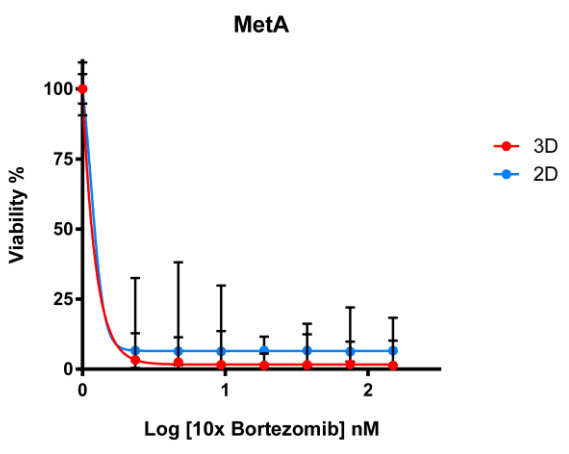

Figure 33. Dose effect of proteasome inhibitor Bortezomib on 2D and 3D cells viability upon 72h. Bortezomib appears to be very effective even for minimal concentrations.

The IKK-2 inhibition outcome from the preliminary screen, and the abrupt viability drop observed just in 3D cultures, enhanced the curiosity for the use of other chemicals targeting the same pathway. But, in fact, the use of IKK2 inhibitor VIII had no impact on cells even at higher doses than the commercially recommended to reach IC_{50} (Table 4).

The effects of other drugs were addressed and unexpectedly many of them had no effect on the viability of cells either on 2D and 3D models (Table 4).

TGF-β inhibition had little effect on cells independently of the cell culture method. This is possibly because of the presence of many other GTP-RAS stimulators that assures the persistent activation of downstream pathway leading to deregulated proliferation and cell survival.

Dose curve analysis for LDH-A inhibitors shows no effect on 3D MetA and D lines, which indicates a possible absence of an hypoxic core.

c-Met inhibitors had no effect either on 2D or 3D cultures, emphasizing that not all of the KRAS mutant cell lines rely on Met to overcome the Anoikis process. Literature does not focus on metastatic cells lines, but reports also fail to show Met dependency for MetA line [46].

Rho inhibition on MetA and D lines did not have any effectiveness on both 2D and 3D cultures. Confluence of 2D cells and 3D closed organization may constrain the Rho signalling dependency of these cells, explaining the lack of efficacy for these inhibitors in KRAS mutants.

Moreover, further assays also showed no efficacy or either 2D *vs* 3D differences towards Focal Adhesion Kinase (FAK) inhibitor compounds.

Table 4. IC_{50} values for several inhibitors on 2D and 3D cultures. Little effect could be seen with most of the used inhibitors. Bortezomib easily lead to cells' collapse and no significant differences were observed between 2D and 3D cultures. NA means that cells did not reach IC_{50}. (-) means that the assay was not performed.

IC_{50}		MetA		LKR		D	
Name	**Description**	**2D**	**3D**	**2D**	**3D**	**2D**	**3D**
Bortezomib (nM)	Proteasome inhibitor	0.1	0.1	0.1	0.2	0.2	0.3
IKK2 inhibitor VIII (nM)	IKK-2 inhibitor	NA	NA	-	-	NA	NA
SB-505124 (μM)	TGF-β inhibitor	NA	NA	NA	NA	NA	NA
PF562271 (nM)	FAK inhibitor	NA	NA	NA	NA	-	-
GSK2837808A (nM)	LDH-A inhibitor	NA	NA	NA	NA	-	-
CT04 (μg/μl)	Rho inhibitor	NA	NA	-	-	NA	NA
PHA665752 (nM)	Selective and ATP-competitive inhibitor of c-Met	NA	NA	NA	NA	NA	NA
PF-02341066 (nM)	c-Met and ALK inhibitor	NA	NA	NA	NA	-	-

Results obtained demonstrated no viability differences between 2D and 3D culture methods. This indicates that for all these tested inhibitors there are no strong evidences that using 3D cultures can bring further insight about the outcome in *in vivo* systems.

3.6.2.3- Structural stability inhibitors

The pathway complexity involved in KRAS cancer cells and the negative feedback loops able to compensate the signalling highlight the difficulty on finding a successful therapeutic target.

A different approach was taken using inhibitors that may alter the structural stability of cells. The main characteristic of cancer cells 3D cultures is the overall arrangement similar to *in vivo* tumors. Thereby, disturbing this organization is expected to be more harmful for 3D cultures than 2D. The actin assembly inhibitor Latrunculin had indeed a good effect on LKR and MetA viability cell lines, being the first one quite sensitive especially when cultured as spheroids, whereas monolayer treatment did not reach the IC_{50} (Figure 34).

A similar effect was encountered with Paclitaxel, a tubulin polymerization promoter and stabilizer already used in clinic. Very promising results were achieved for MetA cell line, with positive 3D sensitiveness disregarding the cytostatic effects on 2D cultures (Figure 34). Such difference cannot be found for LKR and D lines which indicates a cell line-dependent drug sensitivity (Table 5).

The half-life of these compounds may also play an important role on the outcome of these end-point assays, and once its effects were just monitored upon 72h treatments, resistance and recovery is likely to happen.

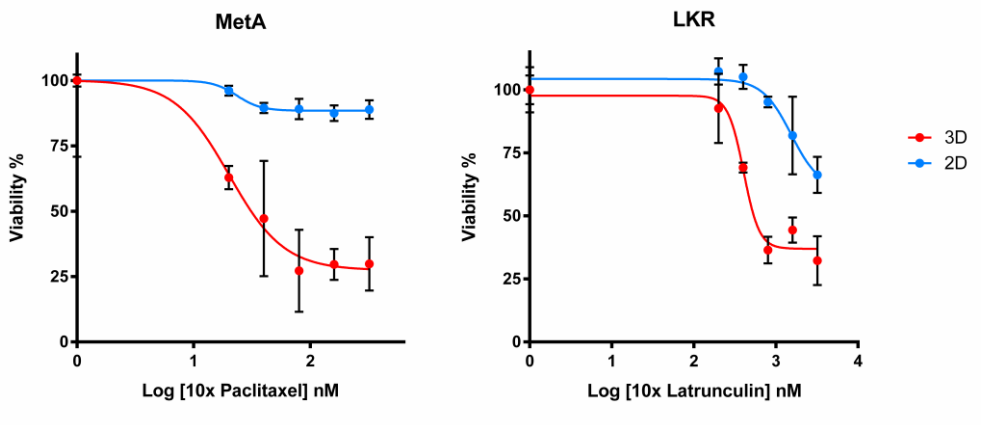

Figure 34. Dose effect of Paclitaxel and Latrunculin on 2D and 3D viability upon 72h treatment. A clear different response is observed for MetA line when treated with the tubulin stabilizer. While there is a drop on spheres viability, 2D cultures are not affected. Similar effect can be seen for LKR with the actin inhibitor. This cell line is more sensitive in 3D than 2D cultures.

Table 5. IC_{50} values for Paclitaxel and Latrunculin on 2D and 3D cultures. MetA 3D cultures are significantly more sensitive to Paclitaxel then 2D. LKR 3D also shows a lower IC_{50} towards Latrunculin treatment. NA means that cells did not reach IC_{50}. (-) means that the assay was not performed.

IC_{50}		MetA		LKR		D	
Name	**Description**	**2D**	**3D**	**2D**	**3D**	**2D**	**3D**
Paclitaxel (nM)	Tubulin polymerization promoter and stabilizer	NA	3	NA	NA	NA	NA
Latrunculin (nM)	Actin assembly inhibitor	155	90	NA	55	-	-

Results obtained indicate that inhibitors that interfere with cell structure are more successful in 3D cultures. The spatial cell organization has then an important role in the effective response of these inhibitors.

In general, these preliminary assays showed that 2D and 3D drug responses are cell line dependent. Differences between culture methods are not clear for several of the tested inhibitors. Only the D line, when cultured under 3D, appears to be more sensitive to inhibitors that target effector proteins of the KRAS pathway. Interestingly, this is the only cell line that showed differentiation functions and a very organized structure. For the other two cell lines, LKR and MetA, differences can only be observed with structural stabilizing inhibitors, which have a big impact in 3D cell viability (Table 6).

This demonstrates the importance of exploring in future work the impact of cells organization and stabilization in cell survival. Moreover, it is also important to bear in mind that cell organization and differentiation affects the way cells react towards pathway inhibitors, as can be observed with the D line.

Table 6. Overview of the culture method that confers the highest sensitivity towards the corresponding drug. 3D cultures for D line confer more sensitiveness upon inhibition of proteins involved in the signal transduction. 3D cultures for MetA and LKR just have a bigger impact on viability with structural stabilizing inhibitors. NA means that cells did not reach IC_{50}. ND means that there are no differences between 2D and 3D. * means that the difference between 2D and 3D is not very significant, the highest IC_{50} divided by the lowest IC_{50} is less than 2.

Higher sensitiveness				
Name	**Description**	**MetA**	**LKR**	**D**
BMS-345541 (μM)	IKK-β (IKK-2/IKBKB) inhibitor	2D	2D	2D*
Gö7874 (μM)	PKC inhibitor	2D*	2D	2D
PD0332991 dihydrochloride (μM)	CDK inhibitor - high selectivity for CDK4 and CDK6	3D*	2D	3D
Trametinib (nM)	MEK inhibitor	2D*	2D	3D
GDC941 (nM)	PI3K inhibitor	2D	2D	3D
Bortezomb	Proteasome inhibitor	ND	2D	2D*
Paclitaxel (nM)	Tubulin polymerization promoter and stabilizer	3D	NA	NA
Latrunculin (nM)	Actin assembly inhibitor	3D*	3D	NA

3.6.2.4- KRAS sensitivity to combined targeted therapies

Concerning the previous results, further tests were done comparing 2D and 3D cultures regarding this time the effect of combined therapies. The results are preliminary and further tests are needed with the drugs alone to confirm the results and have higher statistical significance.

In overall, no additional effect can be observed with the combination of mTOR inhibitors with CDK inhibitors and no differences exist between both culturing methods (Table 7).

Assays blocking effects of KRAS mutant constitutive pathway activation with PI3K and MEK inhibitors have already proven to bring more sensitiveness to 2D cultures for LKR and MetA lines. Combination of both inhibitors brought down the viability of LKR spheres to the same level as in 2D cultures (Figure 35), which possibly indicates a better outcome for cells cultured in 3D when therapies are combined, bringing promising perspectives to *in vivo* assays (Table 7).

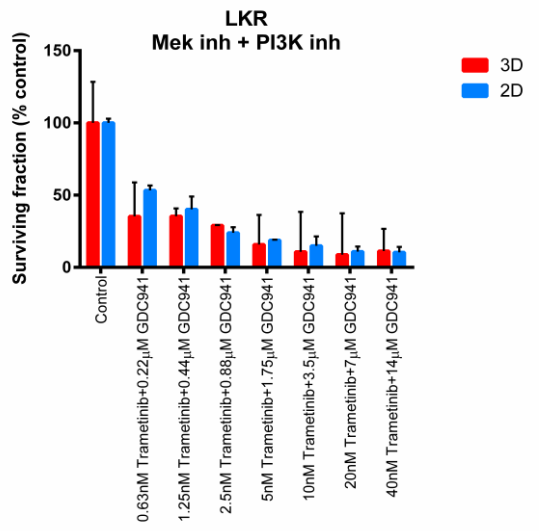

Figure 35. Dose effect of combined MEK and PI3K inhibitors on 2D and 3D viability upon 72h treatment. A bigger impact is noticed on LKR 3D cultures when MEK and PI3K inhibitors are combined, compared with the single treatment shown in Figure 31.

Table 7. Therapy combinations. The percentage of the end point viability reached by cells is represented upon increasing dose treatments. Comparisons can be made looking at the drugs effect alone. MEK and PI3K inhibition had higher effectiveness when combined for LKR in 3D.

End point viability %		MetA		LKR		D	
Name	**Description**	**2D**	**3D**	**2D**	**3D**	**2D**	**3D**
PD0332991 dihydrochloride (μM)		42	31	31	48	76	48
PD0332991 dihydrochloride (μM) + AZD8055 (nM)	CDK + mTOR inhibitors	25	36	49	33	42	64
GDC941 (nM)		16	16	5	38	30	27
Trametinib (nM)		23	17	10	46	20	9
Trametinib (nM) + GDC941 (nM)	MEK + PI3K inhibitors	12	9	10	9	18	8

KRAS mutants are very sensitive to the proteasome inhibitor Bortezomib both in 2D and 3D. In this sense, the Bortezomib IC_{20} dose was combined with IKK-β and MEK inhibitors. A big viability decrease was mainly observed for LKR 3D cultures, but 2D is still more sensitive (Figure 36, Table 8).

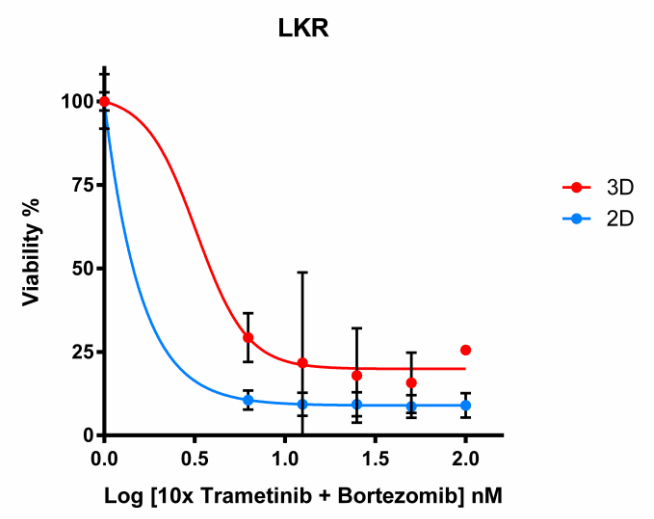

Figure 36. Dose effect of Trametinib combined with the corresponding IC_{20} dose for Bortezomib on 2D and 3D viability upon 72h treatment. A bigger impact is noticed on 3D cultures when MEK and proteasome inhibitors are combined.

Table 8. IC_{50} for therapy combinations. Drugs effect when alone or combined. A significant decrease on LKR 3D cultures happens when Bortezomib IC_{20} dose is added to Trametinib.

	MetA		LKR		D	
Name	**2D**	**3D**	**2D**	**3D**	**2D**	**3D**
BMS-345541 (μM)	0.6	1.1	1.6	2.3	1.2	1.4
Trametinib (nM)	0.5	0.6	0.3	43	1	0.4
Bortezomib (nM)	0.1	0.1	0.1	0.2	0.2	0.3
BMS-345541 (μM) + Bortezomib (nM)	0.1	0.1	0.2	0.5	0.2	0.5
Trametinib + Bortezomib (nM)	0.1	0.2	0.1	0.4	0.1	0.2

Results are still preliminary, therefore conclusions about the synergistic effect of combined therapies will require further analysis.

3.7- MEK inhibition resistance

Attempts from other lab members to generate Trametinib resistant cell lines have been made. We tried to generate resistant cells using the 3D cultures and then compare the sensitivity in 2D and 3D. For this purpose, 10 day treatment of 3D cultures with Trametinib and reseeding on 2D and 3D cultures again, generated cultures less sensitive to Trametinib. However, 2D and 3D cultures were equally affected (Figure 37, Table 9).

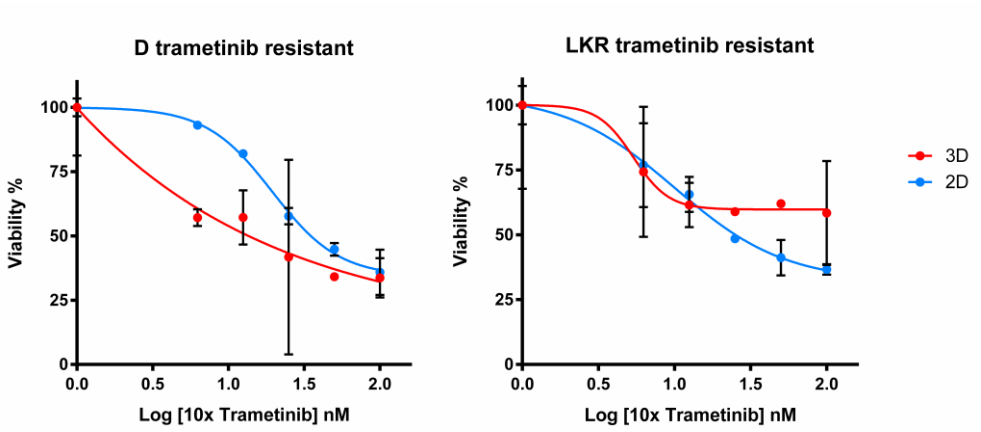

Figure 37. Dose effect of Trametinib on 2D and 3D Trametinib resistant cells upon 72h treatment. For both cell lines and both culture methods long periods of Trametinib exposure induces cells resistance turning them less sensitive to the MEK inhibitor.

Table 9. IC_{50} for 2D and 3D Trametinib resistant cells. IC_{50} increases after long periods with Trametinib treatment. NA means that cells did not reach IC_{50}.

	LKR		D	
Name	**2D**	**3D**	**2D**	**3D**
Trametinib (nM)	0.3	43	1	0.4
Trametinib Resistant	2.5	NA	3.5	1.4

Most likely longer treatment periods will be necessary to result in a more resistant model.

It was previously shown that tumor spheroids are excellent models to study antitumor drug resistance [60]. It would then be interesting to explore whether cell organization in 3D has any influence in the acquisition of resistance upon certain treatments.

3.8- KRAS knockdown spheres

Our final objective was to use small interfering RNA (siRNA) to manipulate gene expression and generate, in spheres, a stable knockdown selective for oncogenic *KRAS*. Cells are generally dependent on KRAS mutant and its knockdown is known to influence cell viability. A stable model would work as a control in future drug assays to interpret how susceptible WT *KRAS* cells are towards the same tested treatments [51].

As described in detail in material and methods, three different approaches were used to knockdown oncogenic *KRAS* in 3D cultures. DharmaFECT transfection reagents were used in already established spheres with 48h and in cells right before seeding spheres. Both methods had no impact on cell growth after 3 days, indicating a deficient transfection despite the use of high siRNA concentrations (Figure 38). In the first case transfection might have been blocked to penetrate the spheres due to the dense matrigel composition, whereas in the second trial transfection appeared to be toxic and did not allow spheres to form.

The same situation was observed with the Oligofectamine transfection reagent which was used to transfect 2D cells before its transfer into 3D cultures (Figure 38). The positive cell survival in both Scramble control and siRNA

KRAS pool shows that, possibly, mainly non-transfected cells were used to form spheres. Lysates from this technique were collected and await for qPCR analysis in order to confirm the efficient transfection.

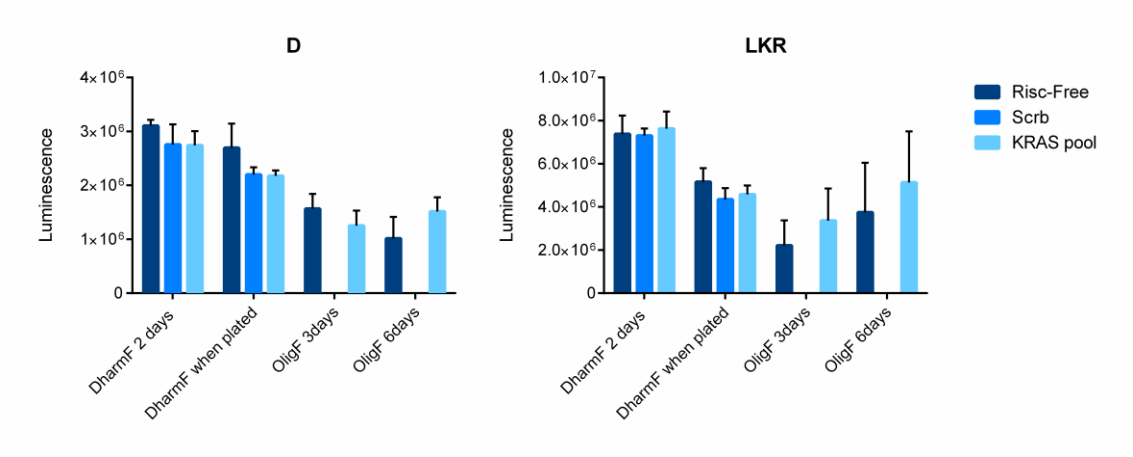

Figure 38. Viability of spheres after different transfection methods. The constant luminescence signal between the controls Risc-Free and Scramble and the siRNA KRAS pool samples shows the deficient transfection.

siRNA transfection in spheres has shown to be more challenging than expected, and further efforts are required to achieve a successful knockdown. Exploring the use of a KRAS inducible system would therefore overcome transfection issues and it is surely not discarded from future directions.

Chapter **4**

Concluding Remarks

3D culture systems are well known for their ability to better mimic *in vivo* conditions. They are able to recreate features of the tumor biology, better predicting therapeutic outcomes. However, the use of this kind of platform for NSCLC cells driven by the mutant KRAS, has not been much explored to the date.

Here we show that KRAS mutant cells from a mouse model are able to grow and survive particularly better in matrix embedded systems. Matrigel 2.5% (v/v) confers the appropriate conditions to culture these cells and is simultaneously suitable for large-scale high throughput screenings, as was also shown by a preliminary screen. CellTiter-Glo assay also showed to be an accurate and sensitive method to monitor cell viability. Its lysing properties are indicated to penetrate the spheres.

Morphologically, spheroids have a very smooth out-layer and tend to form adhesion complexes between cells. Cell cross communication with factors or stimulus may then occur at a higher level in 3D cultures. TEM images showed particular differentiation features in the D cell line. It is a very well organized structure that forms defined acini and is positive for E-cadherin.

Evaluation of the pathway activation showed a persistent increase in the activity of p-ERK on 3D cultures for all of the tested cell lines. However, the culture system does not seem to have an influence on the activity of other proteins such as p-AKT and p-MLC, which showed no apparent variation.

Differences on KRAS dependencies between 2D and 3D cultures were also subject of study. We targeted KRAS downstream effectors or other pathways

that have been shown to play a role on the survival of cells harboring KRAS mutations. Results showed that there are some differences in drug sensitivity between both 2D and 3D settings, but that they are usually cell line dependent.

Differences are especially evident for the D line. This cell is apparently more sensitive to inhibitors like CDK, MEK and PI3K when cultured in 3D, whereas the opposite happens for the MetA and LKR lines, which are more responsive in 2D for the same targets of the KRAS pathway.

On the other hand, MetA and LKR spheroids showed a good response towards structural stability inhibitors like Paclitaxel and Latrunculin, while it was ineffective for 2D cultures and the D line both in 2D and 3D settings.

The results obtained also suggest that it may be an important link between spheroid structural organization and its responsiveness and that this link is worth to be explored further. Interestingly, the D line, which displayed the most well organized 3D structure, is the only one that is more vulnerable to KRAS pathway targets in a 3D setting. On the other side, MetA and LKR lines, which showed to be 3D randomly organized, are the most sensitive to structural stability inhibitors.

In summary, we have developed a method to grow NSCLC cell lines in 3D and quantify cell viability after drug treatment. Results demonstrate that 2D and 3D cultures show different sensitivity to certain inhibitors. Therefore, testing automatically large sets of drugs may eventually highlight new exclusive 3D targets that will reflect better the drug response in an *in vivo* setting. 3D cultures are then promising tools with potential to contribute for the development of new anti-cancer agents in the future.

References

[1] S. Luo, M. Sun, R. Jiang, G. Wang, and X. Zhang, "Establishment of primary mouse lung adenocarcinoma cell culture," *Oncol. Lett.*, vol. 2, pp. 629–632, 2011.

[2] F. Ferlay J, Soerjomataram I, Ervik M, Dikshit R, Eser S, Mathers C, Rebelo M, Parkin DM, Forman D, Bray, "Lung Cancer Estimated Incidence, Mortality and Prevalence Worldwide in 2012," *GLOBOCAN 2012 v1.0, Cancer Incid. Mortal. Worldw. IARC CancerBase No. 11 [Internet].*, pp. 1–6, 2013.

[3] J. M. Fritz, L. D. Dwyer-Nield, and A. M. Malkinson, "Stimulation of neoplastic mouse lung cell proliferation by alveolar macrophage-derived, insulin-like growth factor-1 can be blocked by inhibiting MEK and PI3K activation.," *Mol. Cancer*, vol. 10, no. 1, p. 76, 2011.

[4] J. O. Hiroko Endo, "Spheroid Culture of Primary Lung Cancer Cells with Neuregulin 1/HER3 Pathway Activation," vol. 8, no. 2, pp. 131–139, 2013.

[5] H. Xie, J. I. Hanai, J. G. Ren, L. Kats, K. Burgess, P. Bhargava, S. Signoretti, J. Billiard, K. J. Duffy, A. Grant, X. Wang, P. K. Lorkiewicz, S. Schatzman, M. Bousamra, A. N. Lane, R. M. Higashi, T. W. M. Fan, P. P. Pandolfi, V. P. Sukhatme, and P. Seth, "Targeting lactate dehydrogenase-A inhibits tumorigenesis and tumor progression in mouse models of lung cancer and impacts tumor-initiating cells," *Cell Metab.*, vol. 19, no. 5, pp. 795–809, 2014.

[6] A. Naalsund, H. Rostad, E. H. Strøm, M. B. Lund, and T.-E. Strand, "Carcinoid lung tumors--incidence, treatment and outcomes: a population-based study.," *Eur. J. Cardiothorac. Surg.*, vol. 39, no. 4, pp. 565–569, 2011.

[7] W. D. Travis, "Update on small cell carcinoma and its differentiation from squamous cell carcinoma and other non-small cell carcinomas," *Mod. Pathol.*, vol. 25, no. S1, pp. S18–S30, 2012.

[8] G. C. Jones, J. D. Kehrer, J. Kahn, B. N. Koneru, R. Narayan, T. O. Thomas, K. Camphausen, M. P. Mehta, and A. Kaushal, "Primary Treatment Options for High-Risk/Medically Inoperable Early Stage NSCLC Patients," *Clin. Lung Cancer*, 2015.

[9] S. Rothschild, "Targeted Therapies in Non-Small Cell Lung Cancer—Beyond EGFR and ALK," *Cancers (Basel).*, vol. 7, no. 2, pp. 930–949, 2015.

[10] M. W. R. Roger J. B. King, *Cancer Biology*, Third. Harlow, England: Pearson Education, 2006.

[11] I. a. Prior, P. D. Lewis, and C. Mattos, "A comprehensive survey of ras mutations in cancer," *Cancer Res.*, vol. 72, pp. 2457–2467, 2012.

[12] J. Downward, "RAS's cloak of invincibility slips at last?," *Cancer Cell*, vol. 25, no. 1, pp. 5–6, 2014.

[13] M. Schwartz, "Rho signalling at a glance," *J Cell Sci*, vol. 117, pp. 5457–5458, 2004.

[14] C. V. Pecot, S. Y. Wu, S. Bellister, J. Filant, R. Rupaimoole, T. Hisamatsu, R. Bhattacharya, a. Maharaj, S. Azam, C. Rodriguez-Aguayo, a. S. Nagaraja, M. P. Morelli, K. M. Gharpure, T. a. Waugh, V. Gonzalez-Villasana, B. Zand, H. J. Dalton, S. Kopetz, G. Lopez-Berestein, L. M. Ellis, and a. K. Sood, "Therapeutic Silencing of KRAS Using Systemically Delivered siRNAs," *Mol. Cancer Ther.*, vol. 13, no. 12, pp. 2876–2885, 2014.

[15] J. Downward, "Targeting RAS signalling pathways in cancer therapy.," *Nat. Rev. Cancer*, vol. 3, no. January, pp. 11–22, 2003.

[16] S. Eser, a Schnieke, G. Schneider, and D. Saur, "Oncogenic KRAS signalling in pancreatic cancer.," *Br. J. Cancer*, vol. 111, no. 5, pp. 1–6, 2014.

[17] D. S. Bassères, A. Ebbs, P. C. Cogswell, and A. S. Baldwin, "IKK is a therapeutic target in KRAS-Induced lung cancer with disrupted p53 activity.," *Genes Cancer*, vol. 5, no. 1–2, pp. 41–55, 2014.

[18] J. K. Won, H. W. Yang, S. Y. Shin, J. H. Lee, W. Do Heo, and K. H. Cho, "The crossregulation between ERK and PI3K signaling pathways determines the tumoricidal efficacy of MEK inhibitor," *J. Mol. Cell Biol.*, vol. 4, no. 3, pp. 153–163, 2012.

[19] E. J. Haagensen, S. Kyle, G. S. Beale, R. J. Maxwell, and D. R. Newell, "The synergistic interaction of MEK and PI3K inhibitors is modulated by mTOR inhibition.," *Br. J. Cancer*, vol. 106, no. 8, pp. 1386–94, 2012.

[20] E. Aksamitiene, A. Kiyatkin, and B. N. Kholodenko, "Cross-talk between mitogenic Ras / MAPK and survival PI3K / Akt pathways : a fine balance," *Biochem. Soc. Trans.*, pp. 139–146, 2012.

[21] M. Molina-Arcas, D. C. Hancock, C. Sheridan, M. S. Kumar, and J. Downward, "Coordinate direct input of both KRAS and IGF1 receptor to activation of PI3 kinase in KRAS -mutant lung cancer," *Cancer Discov.*, vol. 3, no. 5, pp. 548–563, 2013.

[22] J. Downward, "RAS Synthetic Lethal Screens Revisited: Still Seeking the Elusive Prize?," *Clin. Cancer Res.*, vol. 21, no. 8, pp. 1802–1809, 2015.

[23] M. Steckel, M. Molina-Arcas, B. Weigelt, M. Marani, P. H. Warne, H. Kuznetsov, G. Kelly, B. Saunders, M. Howell, J. Downward, and D. C. Hancock, "Determination of synthetic lethal interactions in KRAS oncogene-dependent cancer cells reveals novel therapeutic targeting strategies," *Cell Res.*, vol. 22, no. 8, pp. 1227–1245, 2012.

[24] Y. Wang, V. N. Ngo, M. Marani, Y. Yang, G. Wright, L. M. Staudt, and J. Downward, "Critical role for transcriptional repressor Snail2 in transformation by oncogenic RAS in colorectal carcinoma cells.," *Oncogene*, vol. 29, no. 33, pp. 4658–4670, 2010.

[25] R. a Vertrees, M. McCarthy, T. Solley, V. L. Popov, J. Roaten, M. Pauley, X. Wen, and T. J. Goodwin, "Development of a three-dimensional model of lung cancer using cultured transformed lung cells.," *Cancer Biol. Ther.*, vol. 8, no. January 2015, pp. 356–365, 2009.

[26] R. & K.-S. Friedrich, J., Ebner, "Experimental anti-tumor therapy in 3-D: spheroids - old hat or new challenge?," *Int. J. Radiat. Biol*, vol. 83, pp. 849–871, 2007.

[27] F. Hirschhaeuser, H. Menne, C. Dittfeld, J. West, W. Mueller-Klieser, and L. a. Kunz-Schughart, "Multicellular tumor spheroids: An underestimated tool is catching up again," *J. Biotechnol.*, vol. 148, no. 1, pp. 3–15, 2010.

[28] J. Friedrich, C. Seidel, R. Ebner, and L. a Kunz-Schughart, "Spheroid-based drug screen: considerations and practical approach.," *Nat. Protoc.*, vol. 4, no. 3, pp. 309–324, 2009.

[29] S. Schmidt, I. Messner, A. C. Luca, S. Mersch, S. E. Baldus, W. Huckenbeck, R. P. Piekorz, W. T. Knoefel, A. Krieg, and N. H. Stoecklein, "Impact of the 3D Microenvironment on Phenotype , Gene Expression , and EGFR Inhibition of Colorectal Cancer Cell Lines," vol. 8, no. 3, 2013.

[30] J. E. Ekert, K. Johnson, B. Strake, J. Pardinas, S. Jarantow, R. Perkinson, and D. C. Colter, "Three-dimensional lung tumor microenvironment modulates therapeutic compound responsiveness in vitro - Implication for drug development," *PLoS One*, vol. 9, no. 3, pp. 1–14, 2014.

[31] R. Lama, L. Zhang, J. M. Naim, J. Williams, A. Zhou, and B. Su, "Development, validation and pilot screening of an in vitro multi-cellular three-dimensional cancer spheroid assay for anti-cancer drug testing," *Bioorganic Med. Chem.*, vol. 21, no. 4, pp. 922–931, 2013.

[32] C. Wang, Z. Tang, Y. Zhao, R. Yao, L. Li, and W. Sun, "Three-dimensional in vitro cancer models: a short review.," *Biofabrication*, vol. 6, p. 022001, 2014.

[33] M. J. Weigelt, B., Ghajar, C. M., & Bissell, "The need for complex 3D culture models to unravel novel pathways and identify accurate biomarkers in breast cancer.," *Adv. Drug Deliv. Rev.*, vol. 69–70, pp. 42–51, 2014.

[34] Promega corporation, "Protocols and applications guide: Cell viability," vol. 23, pp. 1–23.

[35] J. S. Sebolt-Leopold and R. Herrera, "Targeting the mitogen-activated protein kinase cascade to treat cancer.," *Nat. Rev. Cancer*, vol. 4, no. 12, pp. 937–947, 2004.

[36] J. S. et al. Sebolt-Leopold, "Blockade of the MAP kinase pathway suppresses growth of colon tumors in vivo," *Nat. Med.*, vol. 5, pp. 810–816, 1999.

[37] A. Carnero and J. M. Paramio, "The PTEN/PI3K/AKT Pathway in vivo, Cancer Mouse Models," *Front. Oncol.*, vol. 4, no. September, pp. 1–10, 2014.

[38] C. López-Otín and T. Hunter, "The regulatory crosstalk between kinases and proteases in cancer.," *Nat. Rev. Cancer*, vol. 10, no. 4, pp. 278–292, 2010.

[39] M. Karin, Y. Yamamoto, and Q. M. Wang, "The IKK NF-kappa B system: a treasure trove for drug development.," *Nat. Rev. Drug Discov.*, vol. 3, no. 1, pp. 17–26, 2004.

[40] E. M. Griner and M. G. Kazanietz, "Protein kinase C and other diacylglycerol effectors in cancer.," *Nat. Rev. Cancer*, vol. 7, no. 4, pp. 281–294, 2007.

[41] H. J. Mackay and C. J. Twelves, "Targeting the protein kinase C family: are we there yet?," *Nat. Rev. Cancer*, vol. 7, no. 7, pp. 554–562, 2007.

[42] E. a Musgrove, C. E. Caldon, J. Barraclough, A. Stone, and R. L. Sutherland, "Cyclin D as a therapeutic target in cancer.," *Nat. Rev. Cancer*, vol. 11, no. 8, pp. 558–572, 2011.

[43] J. D. B Weigelt, PH Warne, "PIK3CA mutation, but not PTEN loss of function, determines the sensitivity of breast cancer cells to mTOR inhibitory drugs," *Oncogene*, vol. 30, pp. 3222–3233, 2011.

[44] T. Gui, Y. Sun, A. Shimokado, and Y. Muragaki, "The Roles of Mitogen-Activated Protein Kinase Pathways in TGF- β -Induced Epithelial-Mesenchymal Transition," vol. 2012, no. type I, 2012.

[45] D. A. Chapnick, L. Warner, J. Bernet, T. Rao, and X. Liu, "Partners in crime : the TGF b and MAPK pathways in cancer progression," *Cell Biosci.*, vol. 1, no. 1, p. 42, 2011.

[46] S. Fujita-Sato, J. Galeas, M. Truitt, C. Pitt, a. Urisman, S. Bandyopadhyay, D. Ruggero, and F. McCormick, "Enhanced MET translation and signaling sustains K-Ras driven proliferation under anchorage-independent growth conditions," *Cancer Res.*, vol. 184624, 2015.

[47] A. Hall, "Rho family GTPases.," *Biochem. Soc. Trans.*, vol. 40, pp. 1378–82, 2012.

[48] E. Sahai and C. J. Marshall, "RHO-GTPases and cancer.," *Nat. Rev. Cancer*, vol. 2, no. February, pp. 133–142, 2002.

[49] D. R. Croft and M. F. Olson, "The Rho GTPase effector ROCK regulates cyclin A, cyclin D1, and p27Kip1 levels by distinct mechanisms.," *Mol. Cell. Biol.*, vol. 26, no. 12, pp. 4612–4627, 2006.

[50] K. B. Dunn, M. Heffler, and V. Golubovskaya, "Evolving Therapies and FAK Inhibitors for the Treatment of Cancer," vol. 10, no. 10, pp. 722–734, 2012.

[51] N. Sunaga, D. S. Shames, L. Girard, M. Peyton, J. E. Larsen, H. Imai, J. Soh, M. Sato, N. Yanagitani, K. Kaira, and Y. Xie, "Knockdown of Oncogenic KRAS in Non – Small Cell Lung Cancers Suppresses Tumor Growth and Sensitizes Tumor Cells to Targeted Therapy," *AACR*, vol. 10, no. February, pp. 336–347, 2011.

[52] L. K. N. Nicholas E., Timmins, "Generation of Multicellular Tumor Spheroids by Hanging-Drop Method," pp. 141–151.

[53] et al. Walzl A., Unger C., Kramer N., Unterleuthner D., Scherzer M., "The Resazurin Reduction Assay Can Distinguish Cytotoxic from Cytostatic Compounds in Spheroid Screening Assays," *J Biomol Screen.*, vol. 19, no. 7, pp. 1047–1059, 2014.

[54] A. Ivascu and M. Kubbies, "Rapid generation of single-tumor spheroids for high-throughput cell function and toxicity analysis.," *J. Biomol. Screen. Off. J. Soc. Biomol. Screen.*, vol. 11, pp. 922–932, 2006.

[55] W. Mueller-klieser, "Three-dimensional cell cultures: from molecular mechanisms to clinical applications," *Am. Physiol. Soc.*, 1997.

[56] A. V. P. Rajeev Singhai, Vinayak W Patil, Sanjog R Jaiswal, Shital D Patil, Mukund B Tayade, "E-Cadherin as a diagnostic biomarker in breast cancer," *N Am J Med Sci.*, vol. 3, no. 5, pp. 227–233, 2011.

[57] G. Hatzivassiliou, B. Liu, C. O'Brien, J. M. Spoerke, K. P. Hoeflich, P. M. Haverty, R. Soriano, W. F. Forrest, S. Heldens, H. Chen, K. Toy, C. Ha, W. Zhou, K. Song, L. S. Friedman, L. C. Amler, G. M. Hampton, J. Moffat, M. Belvin, and M. R. Lackner, "ERK Inhibition Overcomes Acquired Resistance to MEK Inhibitors," *Mol. Cancer Ther.*, vol. 11, no. 5, pp. 1143–1154, 2012.

[58] a L. Bishop and a Hall, "Rho GTPases and their effector proteins.," *Biochem. J.*, vol. 348, pp. 241–255, 2000.

[59] B. J. Altman and J. C. Rathmell, "Metabolic Stress in Autophagy and Cell Death Pathways," *Cold Spring Harb. Perspect. Biol.*, vol. 4, pp. a008763–a008763, 2012.

[60] W. Mueller-klieser, "Tumor biology and experimental therapeutics," *Elsevier - Crit. Rev. Oncol. Hematol.*, vol. 36, pp. 123–139, 2000.

Supplementary Information

Supplementary Information 1. D line does not show villi in 2D cultures. Contrarily to 3D cultures, TEM images show the absence of microvilli in the D cell line.

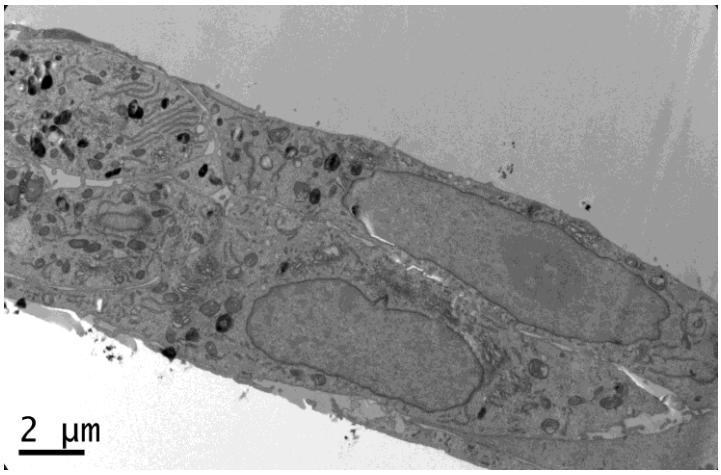

Supplementary Information 2. Drug dose assays. Differences can be observed between 2D and 3D for some inhibitors. However the differences are cell line dependent.

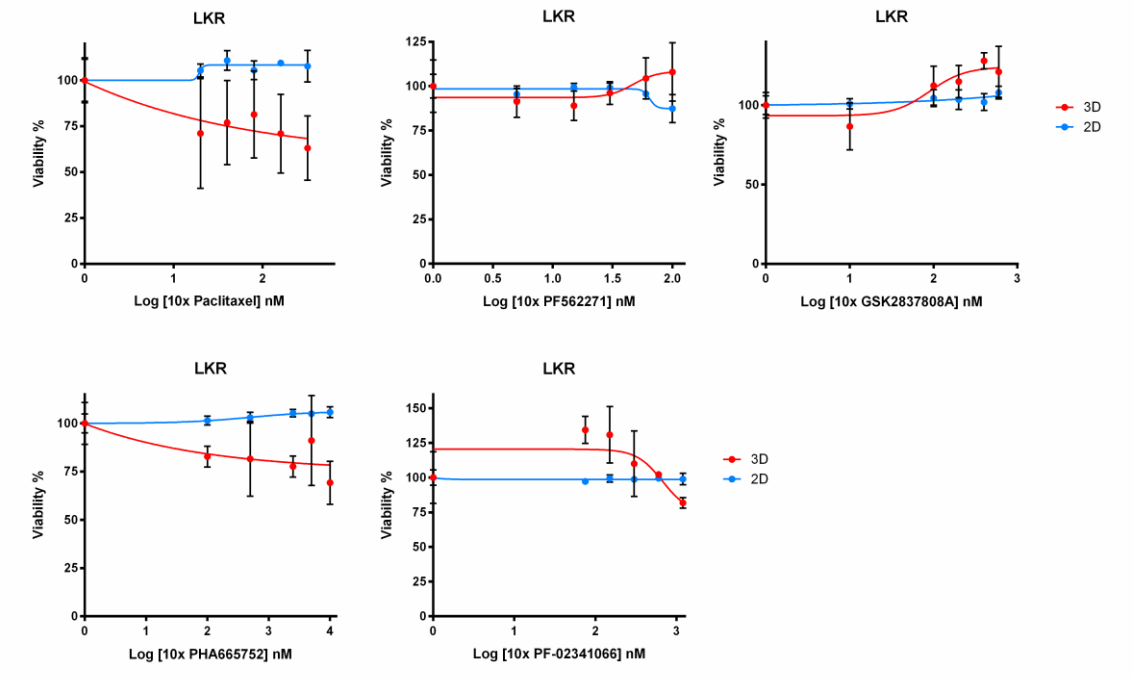

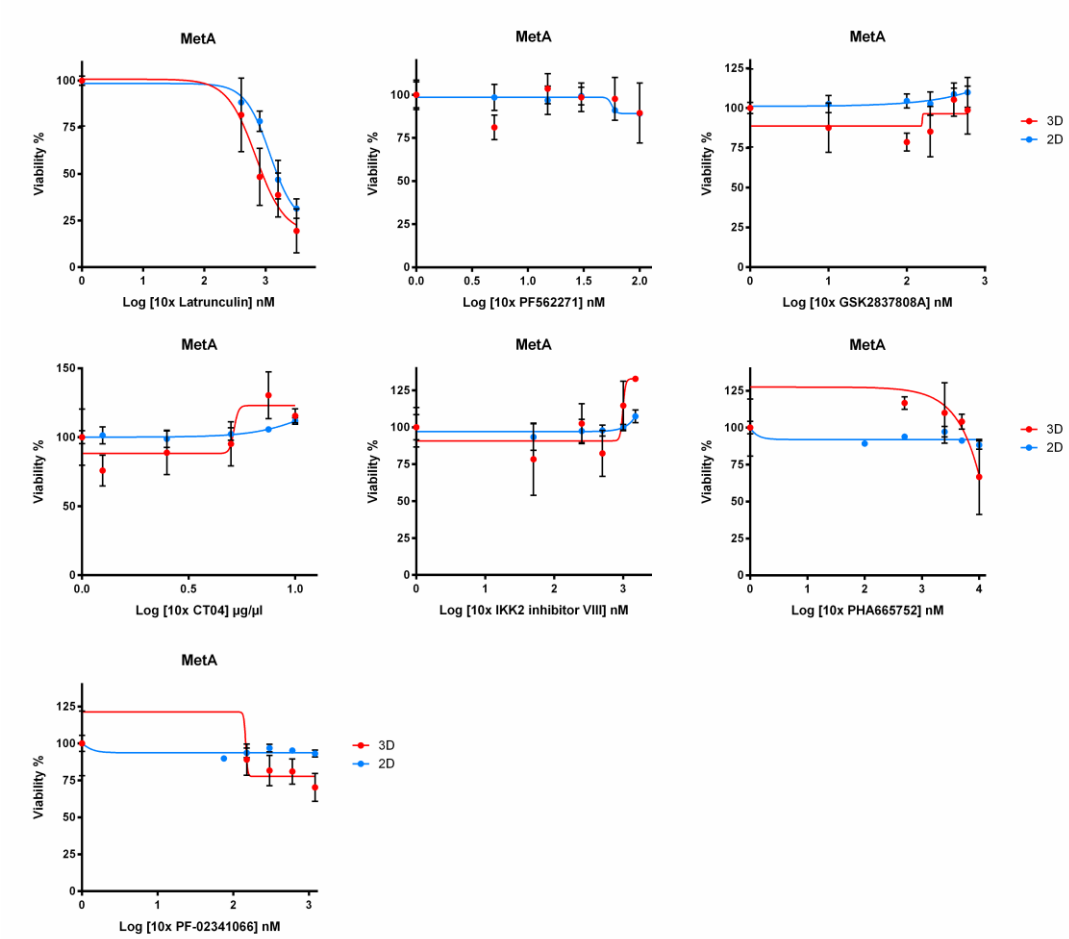
MetA
Viability %
Log [10x Latrunculin] nM
MetA
Viability %
Log [10x PF562271] nM
MetA
Viability %
Log [10x GSK2837808A] nM
3D
2D
MetA
Viability %
Log [10x CT04] µg/µl
MetA
Viability %
Log [10x IKK2 inhibitor VIII] nM
MetA
Viability %
Log [10x PHA665752] nM
3D
2D
MetA
Viability %
Log [10x PF-02341066] nM
3D
2D

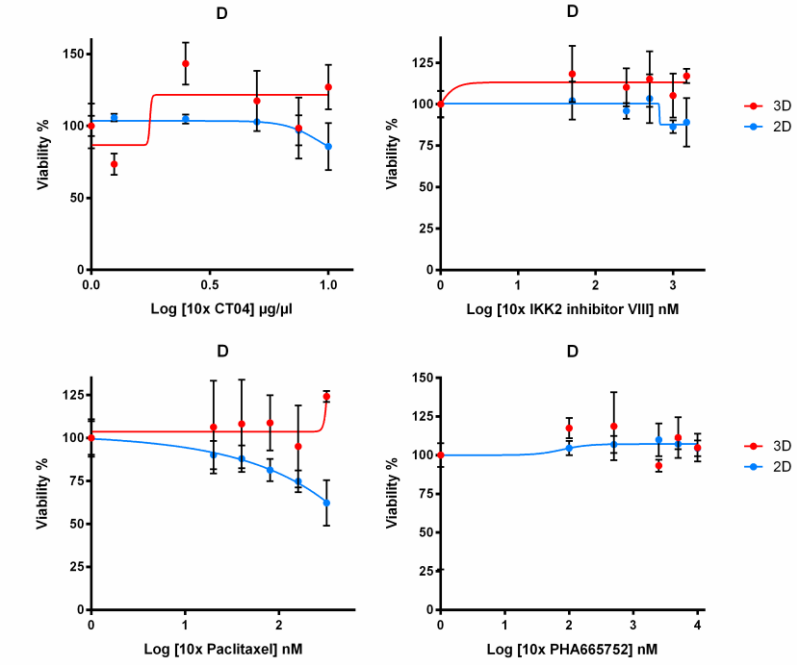
D
Viability %
Log [10x CT04] µg/µl
D
Viability %
Log [10x IKK2 inhibitor VIII] nM
3D
2D
D
Viability %
Log [10x Paclitaxel] nM
D
Viability %
Log [10x PHA665752] nM
3D
2D

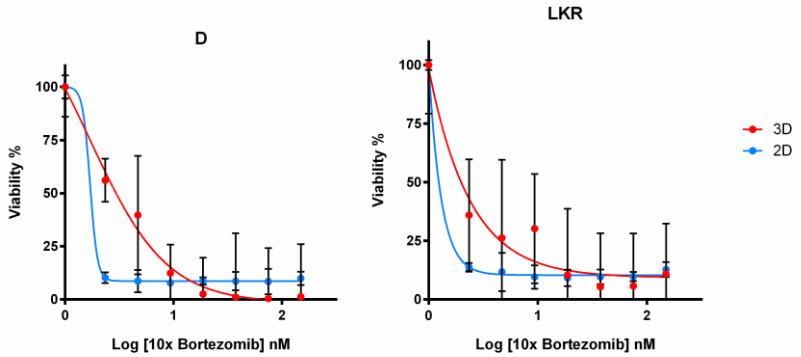
D
LKR
Viability %
Log [10x Bortezomib] nM
3D
2D

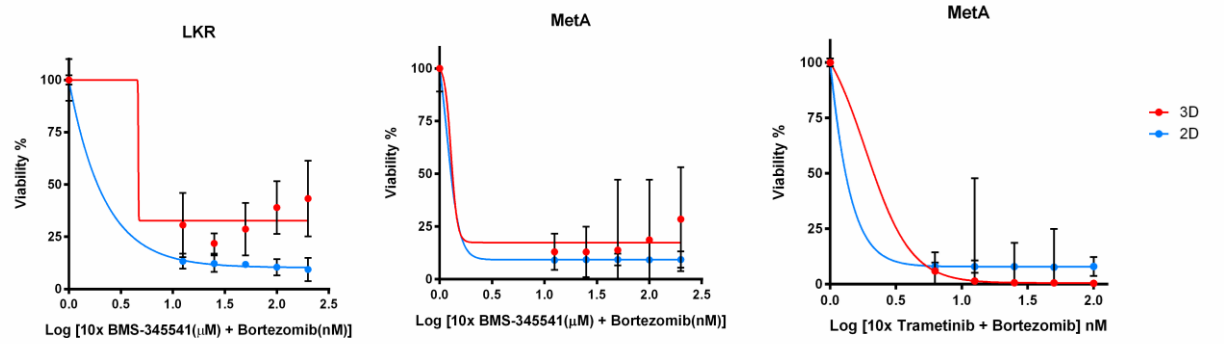
LKR
MetA
MetA
Viability %
Log [10x BMS-345541(μM) + Bortezomib(nM)]
Log [10x Trametinib + Bortezomib] nM
3D
2D

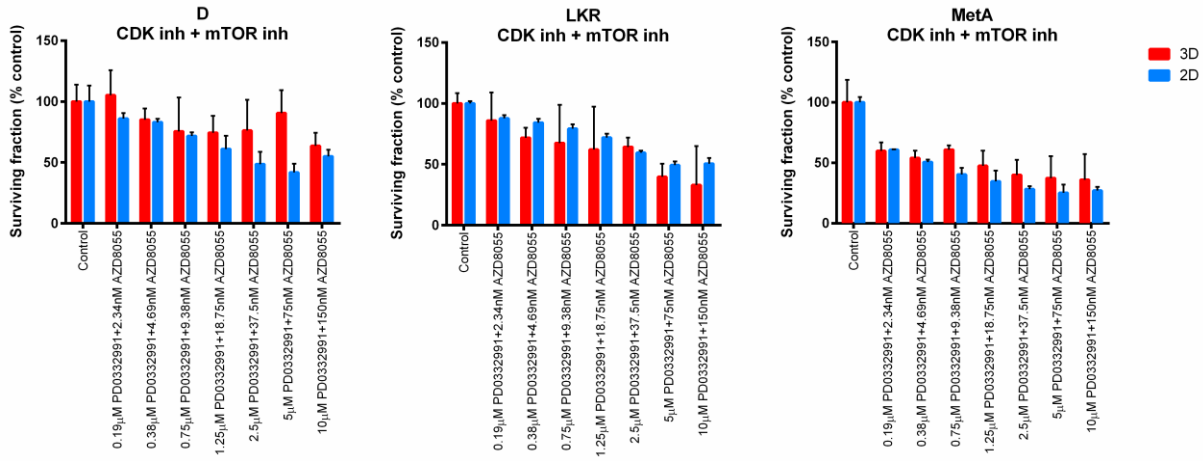
D
CDK inh + mTOR inh
LKR
CDK inh + mTOR inh
MetA
CDK inh + mTOR inh
Surviving fraction (% control)
Control
0.19μM PD0332991+2.34nM AZD8055
0.38μM PD0332991+4.69nM AZD8055
0.75μM PD0332991+9.38nM AZD8055
1.25μM PD0332991+18.75nM AZD8055
2.5μM PD0332991+37.5nM AZD8055
5μM PD0332991+75nM AZD8055
10μM PD0332991+150nM AZD8055
3D
2D

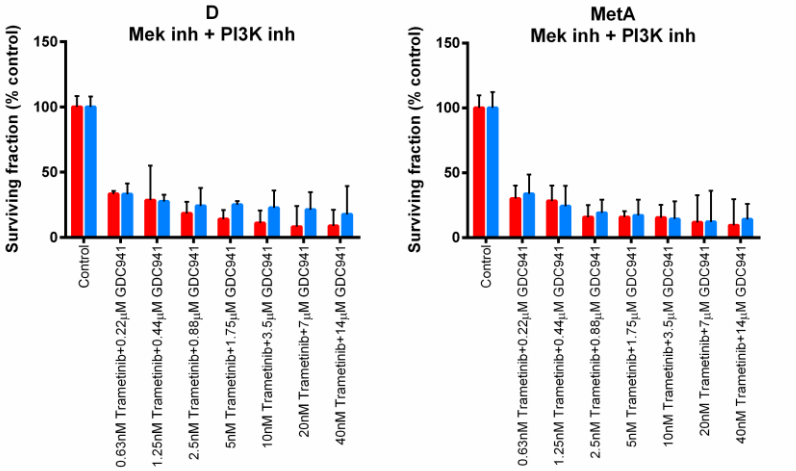
D
Mek inh + PI3K inh
MetA
Mek inh + PI3K inh
Surviving fraction (% control)
Control
0.63nM Trametinib+0.22μM GDC941
1.25nM Trametinib+0.44μM GDC941
2.5nM Trametinib+0.88μM GDC941
5nM Trametinib+1.75μM GDC941
10nM Trametinib+3.5μM GDC941
20nM Trametinib+7μM GDC941
40nM Trametinib+14μM GDC941
3D
2D